THERMOELECTRIC POWER AND DC CONDUCTIVITY OF AMORPHOUS Ge_{10} Si_{12} As_{30} Te_{48} SEMICONDUCTORS

A THESIS

Presented to

The Faculty of Graduate Studies and Research

The University of Manitoba

In Partial Fulfillment

of the Requirement for the Degree of

MASTER of SCIENCE

in

Electrical Engineering

by

Lok Chow

February, 1976

"THERMOELECTRIC POWER AND DC CONDUCTIVITY OF AMORPHOUS Ge_{10} Si_{12} As_{30} Te_{48} SEMICONDUCTORS"

by

LOK CHOW

A dissertation submitted to the Faculty of Graduate Studies of the University of Manitoba in partial fulfillment of the requirements of the degree of

MASTER OF SCIENCE

ACKNOWLEDGEMENT

The author wishes to express his sincere thanks to Professor K.C. Kao for his guidance throughout this research program. Thanks also due to Drs. M. Saji, W. Hwang and K. Nakasima for helpful discussions and to Mr. J. Sill for preparing the experimental apparatus.

ABSTRACT

Amorphous $Ge_{10}Si_{12}As_{30}Te_{48}$ semiconductor samples have been fabricated in a sandwich configuration with molybdenum contacts for dc conductivity measurements and in a rectangular block with indium-copper contacts for thermoelectric power measurements. The dc conductivity has been measured as a function of temperature in the temperature range from 444°K to 161°K at an applied field of 10^5 V/m, and the thermoelectric power has been measured in the temperature range from 400°K to 303°K. The results show that the dc conductivity increases exponentially with increasing temperature, and the activation energies deduced from this temperature dependence are from 0.556 eV to 0.505 eV, and the corresponding pre-exponential factors from 4.25×10^3 ohm^{-1} cm^{-1} to 2.55×10^2 ohm^{-1} cm^{-1}, respectively; and that the thermoelectric power decreases linearly with increasing temperature, and the activation energy deduced from this temperature dependence is about 0.414 eV, and the corresponding temperature factor about 9.2×10^{-6} eV/K. Also, the thermoelectric power is positive indicating a p-type conduction. On the basis of the Mott-CFO model, the possible transport mechanisms are the in-band conduction, the hopping conduction near the valence band edge, and the hopping conduction amongst the localized states to the nearest neighbors.

TABLE OF CONTENTS

LIST OF SYMBOLS

a	interatomic seperation
A	area
β	temperature factor of the activation energy $(E_F - E_v)$
β^*	Thomson coefficient
D	diffusion coefficient
E_c, E_v	the mobility gap edges at the conduction and valence bands
E_F	Fermi energy
E_g	mobility gap (equals to $E_c - E_v$)
ΔE_o	electrical activation energy
ΔE_{opt}	optical band gap
ΔE_s	activation energy of thermoelectric power
ΔE_μ	activation energy of mobility
$f(E)$	Fermi-Dirac distribution function
$\hbar$	reduced Planck's constant $(= h/2\pi)$
P	Peltier coefficient
i_{P_d}	density of the empty valence tail states at energy E_i
Q	the amount of heat transfer
S	thermoelectric power (TEP) or Seebeck coefficient
T	temperature (K°)
t	thickness
v_s	sample voltage
V	dc voltage
W	activation energy for low temperature hopping conduction
ΔW_1	activation energy of the hopping conduction from near band edge energy level into the band

ΔW_2	activation energy of the hopping conduction to the nearest neighbors near E_F
ψ	wavefunction of the carriers
λ	mean free path of the carriers
σ	dc conductivity
$<\sigma_E(o)>$	dc conductivity contributed by the carriers at the energy level E
ω	frequency of the phonon spectrum of the material
ν_{el}	the mean frequency of an electron jumping out of a site
ν_{ph}	the electronic frequency for hopping
τ	relaxation time

LIST OF TABLES

LIST OF FIGURES

CHAPTER 1

INTRODUCTION

Glasses are ancient materials, but through modern science and technology new types and novel applications of these materials have been developed during the last decade. Among different types of glasses semiconducting glasses have very special electrical and optical properties which are of great importance to many engineering applications, such as dielectrics, switching and memory devices, photoreceptors in xerography, etc. Moreover, semiconducting glasses are also of great interest to scientists quite apart from their many practical applications; certain phenomena ocurring in semiconducting glasses lie at the frontier of science and stimulate scientific work of the highest sophistication and quality. For instance, the non-crystalline structure of semiconducting glasses and its relation to their electrical, optical and thermal properties are not well understood; it will become one of the most active and challenging fields in science.

A glass here denotes a non-crystalline or amorphous solid formed by the undercooling of a liquid or by the condensation of a vapor onto a cold substrate. Those glasses having semiconducting properties are usually referred to "non-crystalline semiconductors" or "amorphous semiconductors". Frequently, amorphous semiconductors are classified by their components into three categories:

(i) Oxide glasses: the semiconducting glasses based on transition metal oxides such as V_2O_5 and Fe_3O_4.

(ii) Non-oxide glasses: the most common non-oxide glasses are so-

called chalcogenide glasses containing one of the following components: sulfur, selenium and tellurium.

(iii) oxychalcogenide glasses: the semiconducting glasses formed by co-melting oxides and chalcogenides.

The material which has been used in this thesis is a four component chalcogenide glass so-called("Ovonic glasses")with compositions Si_{10} Ge_{12} As_{30} Te_{48}; which was first used by Ovshinsky for switching devices.

The semiconducting properties of glasses were first reported by Baynton in 1957. From 1957 to about 1964, most of the studies were concentrated on oxide glasses based on transition metal oxides. Before 1964, only elemental selenium had been widely studied among the non-oxide glasses. This is because Se is a high resistivity photoconductor and its characteristics are exploitable in xerographic process. Studies of other chalcogenide glasses were almost exclusively the work of Kolomiets and Pearson around 1964. Kolomiets (1964) found that most of the chalcogenides are of high resistivity (higher than 10^3 ohm-cm at 300°K) and low mobility (less than 1 cm^2/V-sec) semiconductors. From his conductivity measurements, Kolomiets (1964) has reported that the activation energies are of the same order of the optical band gap energy. Pearson and co-workers in the same year have also reported that the sign of the dominated carriers deduced from the thermoelectric power measurements was opposite to that from the Hall effect measurements. More important, he observed the switching phenomena, which later became one of the most interesting subjects in this field.

In the past few years, very widespread studies have been done both theoretically and experimentally on different kinds of chalcogenide glasses.

Among the chalcogenides, the Si-Ge-As-Te system is particularly important since it normally exhibits a very stable and sensitive switching effect with a very short turn-on time. However, the actual process of switching is still not very clear and it is therefore necessary to have more information about the electronic structure and the carrier transport mechanisms in these materials.

The thermoelectric power measurement is important in the studies of amorphous semiconductors simply because it provides the information of the type of predominated carriers, also the thermal activation energy deduced from this measurement bears a definite relation with the optical band gap and the electrical activation energy obtained from dc conductivity measurements. Moreover, thermoelectric power can also provide a rough estimation of the temperature factor of the band gap (Fritzsche 1971). Particularly, the sign of Hall coefficient R_H has been observed to be anormalous in most of the chalcogenides (see, for example, the appendix of "Electronic Processes in Non-crystalline materials", Mott and Davis, 1971), the thermoelectric power measurement seems to be the most reliable method for determining the type of carrier predominated in amorphous materials. However, so far little has been reported about the thermoelectric power measurement on Si-Ge-As-Te system (Rockstad et al., 1972 on Ge_7 Si_{18} As_{35} Te_{40}). It is therefore the purpose of this thesis to present a systematic study on thermoelectric power and electrical conductivity in Si-Ge-As-Te system.

In Chapter 2, a brief survey of the previous research on amorphous semiconductors is given. Since amorphous materials have been extensively studied in the past few years, only those topics which are relevant to the present subjects are included. These topics are

grouped into three parts; Part 1 is a review on the theoretical work of the electronic structure of chalcogenide glasses; such as the mobility gap, the density of states, the distribution of localized states and the electronic model for chalcogenides; Part 2 concerns the dc conductivity and the transport mechanisms and their temperature dependence; and Part 3 the thermoelectric effect and the temperature dependence of the thermoelectric.

The experimental procedures, sample preparation, and the measuring techniques are given in detail in Chapter 3. Chapter 4 gives the experimental results of the temperature dependent dc conductivity and thermoelectric power measurements and a brief discussion on these results. Conclusions and a proposed future research plan are given in the last chapter.

CHAPTER 2

REVIEW OF THE PREVIOUS WORK ON AMORPHOUS SEMICONDUCTORS

PART 1. THE ELECTRONIC STRUCTURE OF AMORPHOUS MATERIALS

Amorphous materials are disordered materials. These materials have some kind of structural defects which disturb the periodicity of the arrangement of atoms and molecules so that the energy bands are seriously perturbated, and the Bloch wave function is no longer an exact solution. The band structure in Wilson-Bloch's sense which is based on the assumption of periodic lattice is therefore violated.

About fifteen years ago, our understanding on disordered materials was still very poor. The electronic structure of crystalline materials is understood by classifying materials into metals, semiconductors and insulators based completely on the band theory in conjunction with a periodic lattice structure. The keys to our present knowledge on amorphous materials have been based on the principle of Ioffe and Regel in 1960, that the mean free path of the carriers can't be less than the distance between atoms; and also on the concept of localization introduced by Anderson in 1958. The theoretical studies on amorphous semiconductors at the present stage are mostly based on these two concepts. We shall start with the relation of these two basic concepts to the important properties of a disordered system, and then discuss the possible electronic model for amorphous materials based mainly on the work of Mott, Cohen and Fritzsche.

2.1. The limitation of Boltzmann equation

The carriers in materials can be affected by external field, temperature gradient,and various scatterings from the impurities, phonons

and carriers themselves. In crystalline materials, the transport properties of carriers is represented by a distribution function $f_{\bar{K}}(\bar{r},t)$, which gives the possible local concentration of carriers in the state $\bar{K}$, in the neighborhood of a point $\bar{r}$ in space, and at time instant t. With the consideration of all the effects acting on the carriers, a transport equation or Boltzmann equation can be set up for $f_{\bar{K}}(\bar{r},t)$. The basic requirement for Boltzmann equation to remain valid is that $f_{\bar{K}}(\bar{r},t)$ must be well defined in $\bar{K}$ space. This has been shown in Bloch theorem that the one-electron wave function in a perfect crystal be of the form

$$\psi(\bar{r}) = \psi_{\bar{K}n}(\bar{r}) = e^{i\,\bar{K}\cdot\bar{r}}\, U_{\bar{K}n}(\bar{r}) \tag{2.1}$$

where the wave vector $\bar{K}$ is in the first Brillouin zone, $U_{\bar{K}n}(\bar{r})$ has the periodicity of the lattice. Equation (2.1) simply means that the wave function has a long range order in phase, and, whenever the phase is given at one point, the phase at any other point in the lattice can be determined if the wave vector $\bar{K}$ is known.

In imperfect crystals, if individual imperfections are randomly distributed, these imperfections will act as scattering centers throughout the material. The wave functions can only be obtained by solving a multiple scattering problem with randomly distributed scattering centers. The solution should be in the form of

$$\psi = \sum_{\bar{K}} a_{\bar{K}}\, \psi_{\bar{K}} \tag{2.2}$$

where the coefficients $a_{\bar{K}}$'s have random phases. The energy of the wave-function ψ will no longer stay on the spherical energy surface in $\bar{K}$ space, but rather would spread out for a small amount ΔK from the surface

because of the uncertainity of the phase. The uncertainty ΔK actually arises from the scattering with the imperfections which can be characterized by the mean free path (the average distance for the wave packet ψ to be scattered). Therefore, the uncertainty ΔK is approximately the reciprocal of the mean free path λ,

$$\Delta K \simeq \frac{1}{\lambda} \tag{2.3}$$

If the concentration of imperfections is not high, the mean free path is large compared with the wavelength of the wavefunction, then we have,

$$\lambda >> \frac{1}{K}, \tag{2.4}$$

and hence

$$\Delta K << K \tag{2.5}$$

The wavefunction can be well defined in $\bar{K}$ space despite of the small uncertainty ΔK as shown in Fig. 2.1. When the density of imperfections increases, the mean free path decreases accordingly and so ΔK becomes large. When the density of imperfection increases beyond a certain value, the lattice loses its periodicity and becomes a disordered system. If the scattering is very strong, the mean free path would reach such a value that the phase of the wave function becomes almost completely random. As emphasized by Ioffe and Regel (1960), the minimum value of λ is about

$$K \lambda_{MIN} \sim 1 \tag{2.5}$$

From equation (2.3), we have

$$\frac{\Delta K}{K} \sim 1 \tag{2.6}$$

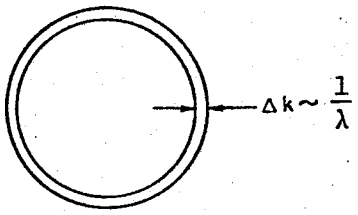

Fig. 2.1. Surfaces of constant $|a_K|$ in K-space (approximate). These coincide with constant energy surfaces in simple cases. The actual surfaces drawn here correspond to the half-maximum values of $|a_K|$; they are separated by $\Delta K \sim 1/\lambda$ where λ is the mean free path. (After Cohen, 1970).

This implies that the uncertainty of K is of the same order of K. The wave vector is no longer a well defined quantity. Physically, when the mean free path is as short as the wave vector, the carriers are mostly characterized by the scattering effect, and lose the wave-like properties. Thus, under such condition, Boltzmann equation loses its validity.

2.2. The localization of states

If the arrangement of atoms and molecules has no periodicity and is completely disordered, then strong potential and state density fluctuation would occur. The density and potential fluctuation will then form traps randomly distributed throughout the system. The energy states of traps in a disordered lattice are generally referred to as localized states (Anderson 1958). The energy state E is localized if an electron with energy between E and $E + dE$ placed in a volume $\Delta\tau$, large enough to satisfy the uncertainty principle, will not deffuse away. On the basis of a potential fluctuated lattice (so-called Anderson lattice) formed by introducing a random potential energy $\frac{1}{2}U$ to a perfect lattice, the localization can then be defined by the ratio U_o/I, where U_o is the measure of the random potential given by

$$U_o^2 = \langle U^2 \rangle , \tag{2.7}$$

and

$$I \simeq e^{-\alpha R} I_o \tag{2.8}$$

and I is the measure of the overlap integral of the wave function in one potential well with its nearest neighbor. The overlap integral should decay spatially from the specified well. The relation between U_o and I can be expressed in the form (Mott and Davis, 1971):

$$\frac{a}{\lambda} = \frac{(U_o/I)^2}{16\pi} \tag{2.9}$$

where a is the interatomic separation.

If the potential fluctuation is small, i.e., U_o is small, the mean free path will be large compared with a. For strong fluctuation, λ must be small compared with a as suggested by Ioffe and Regel, the minimum value of λ is $\lambda_{MIN} \sim a$. Anderson has suggested that $\lambda \sim a$ can be used as the criterion for localization. According to equation (2.9), when (U_o/I) reaches the value approximately equals to 7, λ is about the same order as a, then localization occurs. The Anderson lattice and the wavefunction in Anderson model are shown in Fig. 2.2 and 2.3.

The localized states can also be defined in terms of dc conductivity $< \sigma_E(o) >$ as suggested by Mott and Davis (1971). For a Fermi gas of non-interacting electrons with energy E, we have

$$\lim_{N' \to \infty} < \sigma_E(o) > = 0 \tag{2.10}$$

The dc conductivity $< \sigma_E(o) >$ is contributed by the electrons with energy E averaged over all configurations of the ensemble. N' is the total number of electrons in the system. Equation (2.10) simply means that the localized states are those energy states which have a definite carrier concentration, but have no contribution to the conductivity. That is, the localized state corresponds to a range of energies, in which the density of state is finite but the mobility of the carriers with energies within such a range is zero at $T = 0°K$.

These two definitions of localized states are basically equivalent. However, the localization viewed from conductivity seems more phenomenological. The localization concept supported by many experimental results

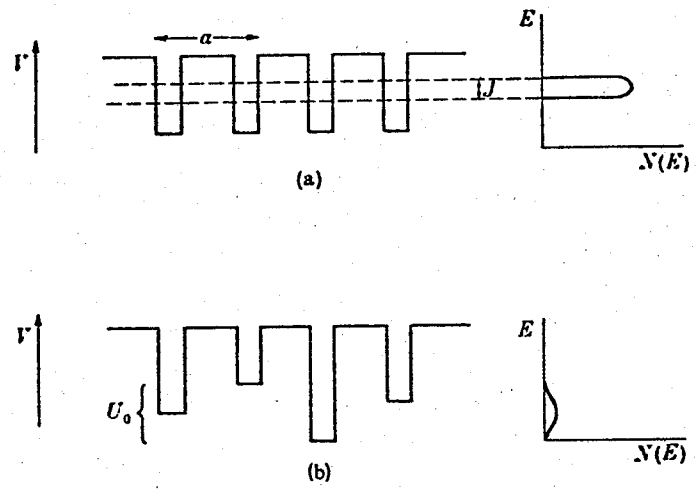

Fig. 2.2. (a) Potential wells for a crystalline lattice, (b) Potential wells for the Anderson lattice. The density of states is shown in both cases. (After Mott and Davis, 1971).

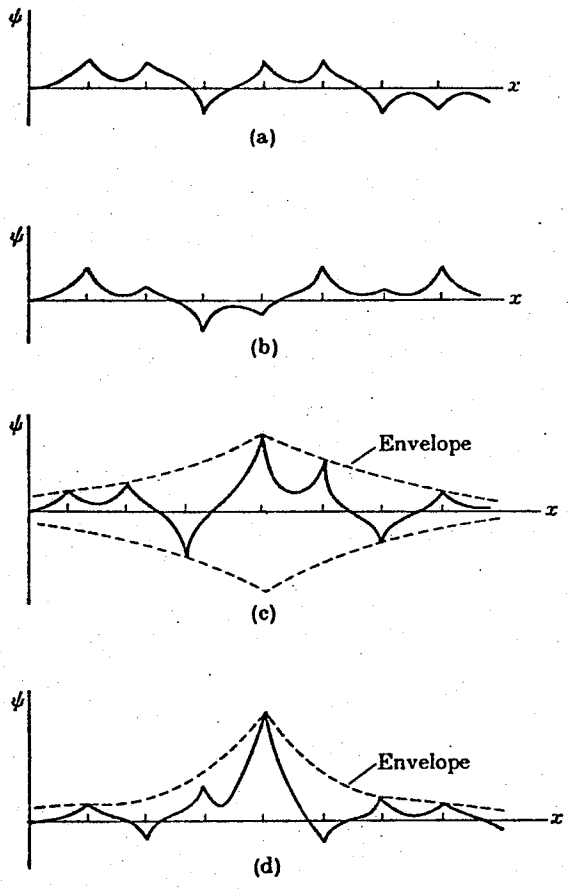

Fig. 2.3. Forms of the wave function in the Anderson model:

(a) When $\lambda \sim a$; (b) when states are just non-localized ($E \geq E_c$); (c) when states are just localized ($E \leq E_c$); (d) strong localization. (After Mott and Davis, 1971).

that there is an extremely large difference in conductivity between amorphous and the corresponding crystalline semiconductors. These results cannot be interpreted just on the basis of energy band separation (J. Tanc and A. Menth 1972). It can be concluded that in a highly disordered system the character of the wavefunction changes and some energy states are localized, so that the wave function and the transport mechanism are different from those for highly ordered (crystalline) systems. The information about the concentration and energy distribution of localized states are very helpful to the understanding of the characteristics and the transport mechanisms of amorphous semiconductors.

2.3. The density of states

Mott and Davis (1971) suggested that the only concept which can be equally applied in both non-crystalline and crystalline state is the density of states. No matter what the nature of the electronic eigenstates can be, the density distribution function must exist. Also, the Fermi-Dirac distribution function

$$f(E) = \frac{1}{\exp(E - E_F)/kT + 1} \tag{2.11}$$

should be valid for disordered system, and thus the Fermi energy E_F can be defined as the limiting value when temperature approaches to zero.

The number of electrons in the energy range between E and $E + dE$ can be expressed as

$$n(E) = N(E)\ f(E)\ dE \tag{2.12}$$

The only quantity which different between amorphous and crystalline states in equation (2.12) is the density of states $N(E)$. In crystalline semi-

conductors, N(E) is deduced from the band theory and is a discrete function with conduction and valence band separated. For semiconductors in amorphous state, band theory is not applicable. N(E) has to be found from different approaches. Mott, Lifshiftz, and those who have been engaged in research in the field of heavily-doped or degenerate crystalline semiconductors, have made a significant contribution towards the understanding of N(E).

The density of states N(E) in amorphous semiconductors can be understood from equation (2.10). This equation implies that some energy range may exist, in which the density of states is finite but localized. Beyond this energy range, the energy states are non-localized (extended), therefore the electrons in these states can contribute to conductivity even at $T = 0°K$. By using Anderson model for a random potential fluctuation lattice in one-dimensional representation as shown in Fig. 2.2, the density of states N(E) is shown schematically in Fig. 2.4. The N(E) distribution curve representing a simple isolated band for electrons consists of a region of extended states for $E_c < E < E_c'$, corresponding to the "conduction band". At the energies E_c and E_c', the character of the energy states changes abruptly from the extended to the localized. These localized state regions are usually referred to the "band tail" of the conduction band. The electrons in extended states are "mobile", and can be referred to as free electrons; the electrons in the tail of conduction band are localized and not easy to diffuse away. Therefore the empty tail states of the conduction band act as electron traps.

According to Anderson's approach, dc conductivity $< \sigma_E(o) >$ at $T = 0°K$ should be in the form as shown in Fig. 2.5. Similarly, we can find the N(E) distribution for holes, with "valence band" in the region

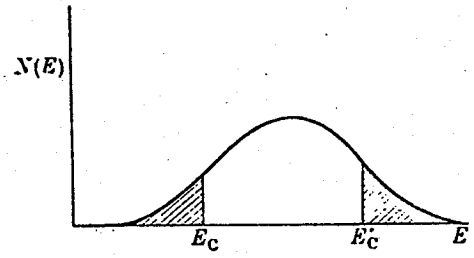

Fig. 2.4. Density of states in the Anderson model. States are non-localized in the centre of the band. Localized states are shown shaded. E_c, E_c' separate the ranges of energies in which states are localized and non-localized. (After Mott and Davis, 1971).

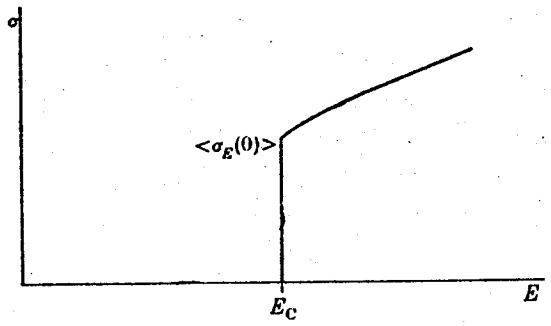

Fig. 2.5. The conductivity $< \sigma_E(o) >$ as a function of E when T = 0 in the Anderson model. (After Mott and Davis, 1971).

$E_v' < E < E_v$, and the localized valence band tail regions beyond E_v' and E_v. The relation between the potential fluctuation and the localized state is shown in Fig. 2.6. Since the "band tailing" is a consequence of fluctuations caused by disoreders, it is reasonable to believe that the higher the degree of disorder, the higher is the concentration of localized states, and thus for a large concentration of localized states the band tail may extend deeper into the band gap.

This simple approach successfully indicates a tentative model for disordered systems. However, since the whole approach is based on the potential fluctuations in the Anderson lattice, it is necessary to consider the density fluctuation which is caused by both translational and compositional disorders in amorphous semiconductors. In amorphous covalent alloys (for example, Si-Ge-As-Te system), the degree of disorders is so high that the band tail states from conduction band and valence band may even overlap (Cohen 1970). The overlapping of band tail states has a very important effect on the behaviour of amorphous covalent alloys in many aspects. The conductivity depends only on two basic quantities: carrier density and mobility; if the carrier density is continuous and has a finite value for all energy levels, then an abrupt change in conductivity with respect to temperature must be resulted from the abrupt change of the mobility. It is reasonable to believe that an energy level must exist at which or in the neighborhood of which the mobility of the carriers abruptly decreases. Under above consideration, the mobility edges E_c and E_v can be defined in terms of dc conductivity. Mott (1967) has suggested that E_c and E_v could be defined by the following relations

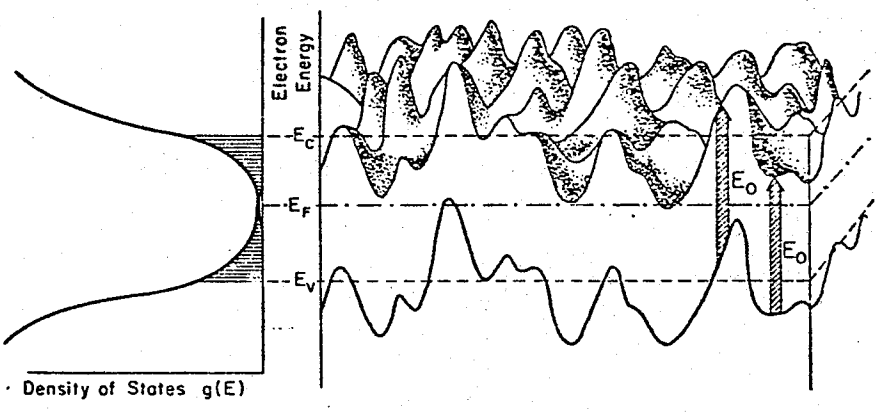

Fig. 2.6. Potential fluctuation of the initial and final electron states for the optical transitions corresponding to the optical gap E_o. The left hand side shows the density of states. The region of localized states lies between E_c and E_v. Note that the short range potential wells which give rise to many of the localized states are not shown here. This figure shows only that part of the long wavelength potential fluctuations which cause a parallel shift of the valence and conduction band states. The part which causes a spatial variation of E_o is omitted for clarity. (After Fritzsche, 1971).

$$\begin{cases} < \sigma_E(o) > = 0 & E < E_c \\ \neq 0 & E > E_c \end{cases} \quad \text{at} \quad T = 0°K \tag{2.13a}$$

$$\begin{cases} < \sigma_E(o) > = 0 & E > E_v \\ \neq 0 & E < E_v \end{cases} \quad \text{at} \quad T = 0°K \tag{2.13b}$$

where E_c and E_v are the mobility edges of conduction band and valence band respectively.

2.4. The mobility structure

Stuke (1969, 1970) was the first to point out that the conductivity of amorphous semiconducting covalent alloys is mostly linearly dependent on temperature in a wide temperature range, and it is associated with a well defined activation energy ΔE_o. On the other hand, the density of states $N(E)$ is a continuous function of E in these materials so that no energy gap could be assumed. It is therefore very difficult to interpret the experimental results by means of energy band structure. Mott (1967) was the first to introduce the concept of mobility edge to separate a range of energy in which states are localized from a range in which it is not. A mobility gap can be defined by mobility edges similar to the energy gap in the band theory. In fact, it is theoretically necessary to assume such a gap to exist in order to explain the observed characteristics of the dc conductivity.

The Fermi energy can be defined by the electroneutrality condition. Since the band tail states retain the charge characteristics from the band from which it is extended, a valence tail state is electrically neutral when it is occupied and a conduction tail state is electrically neutral when it is empty. The location of E_F is such that the number of empty

states in the tail of the valence band above E_F equals the number of occupied states in the tail of the conduction band below E_F. The measurement of electron tunneling through a metal-oxide-amorphous semiconductor system shows that the Fermi energy level is approximately located near the gap center in the temperature range 300°K to 78°K (Cohen, Fritzsche and Ovshinsky 1969). The state density at E_F can be estimated by the measurements of the dc conductivity at low temperatures and is estimated to be 10^{19} to 10^{20} cm^{-3} eV^{-1} (Cohen, Fritzsche and Ovshinsky 1969).

Since the density of states has a finite value within the mobility gap, the gap is usually referred to as the "pseudogap". The mobility for the carriers with energies $E_v < E < E_c$ in the pseudogap is therefore zero at 0°K. Also discontinuities must occur for the mobility at $E = E_c$ and $E = E_v$ at 0°K.

It has been extensively discussed by Mott, Cohen, Anderson, Bronch-Bruevich, Brouers, and Edwards on the definition (2.13a,b) of mobility edges and gap (see, for example, J. Non-cryst. Solids 4 (1970) 391-435). The major two aspects are as follows:

(i) I possible for $\mu(E_F) = 0$ at $T = 0°K$ when $n(E_F)$ is finite in the mobility gap?

(ii) Do discontinuities occur in $\mu(E)$ at $E = E_c$ and $E = E_v$ at $T = 0°K$?

The answers to these two questions are rather speculative. There is no experimental evidence to prove the existence of discontinuities of $\mu(E)$, nor the zero value of $\mu(E_F)$ at $T = 0°K$. Cohen (1970) has emphasized that question (ii) is not essential as long as the mobility edges E_c and E_v can be well defined. He has estimated the mobility

drop within a small energy range about kT near E_c and E_v by assuming two transport mechanisms: phonon-assisted hopping for localized states and propagation with occasional scattering mechanisms for the states which are just non-localized. The lower limit to the mean free path λ for the propagation with occasional scattering mechanism is of the order of interatomic separation (say, 3Å), this correspond to a mobility of 5 cm^2/V sec. The upper limit for hopping conduction would be about 10^{-2} cm^2/V sec. (These two mechanisms will be discussed in Part 2 of this chapter). Therefore, we have a mobility drop of 2.5 orders of magnitude within an energy range kT, which should be enough for a well defined mobility edge E_c. According to previous estimation, Cohen has presumed a continuous but abrupt change of $\mu(E)$ near E_c and E_v, which is somewhat different from Mott's definition (2.13a,b).

As to the first question, Bronch-Bruevich has suggested that $\mu(E_F)$ can't be zero if $n(E_F)$ is finite. However, $\mu(E_F)$ should be very small compared with $\mu(E)$ outside the mobility gap since the carriers in the gap region are localized. The mobility $\mu(E_F)$ may or may not be zero, however, will not affect significantly the mobility gap structure.

The mobility structures at $T = 0°K$ suggested by Mott, Cohen and Bronch-Bruevich are schematically shown in Fig. 2.7, and the mobility at finite termperatures in Fig. 2.8.

2.5. The mobility shoulder - Brownian motion

The mobility $\mu(E)$ drops abruptly within a small energy range about kT near E_c (and E_v) from about 5 cm^2/V sec to 10^{-2} cm^2/V sec. This dropping region is termed the mobility shoulder. Cohen (1970) has suggested that the transport mechanism in this region is quite different from other

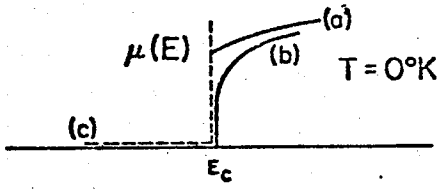

Fig. 2.7. Simple model for the energy dependence of the mobility at T = 0°K. The solid curve (a) was proposed by Mott, shows a discontinuous drop of mobility from finite value to zero. The curve (b) was proposed by Cohen. The mobility drops abruptly but continuously toward zero. The dotted line was proposed by Bronch-Bruevich that the mobility has a finite but small value within the mobility gap. (After Cohen, 1971).

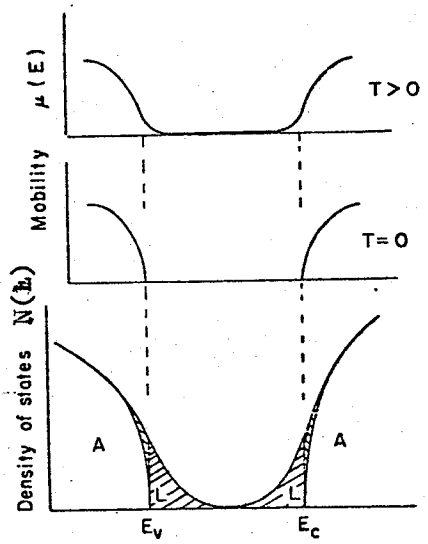

Fig. 2.8. The lower half shows the density of states $N(E)$ as a function of electron energy. Localized states and regions are found between the percolation thresholds E_c and E_v. They coexist in this classical picture with extended channel states for some energy beyond E_c and E_v. At absolute zero the mobility edges are expected to be at E_c and E_v which become less sharp at finite temperatures where phonon assisted hopping can occur between localized regions and states. (After Fritzsche, 1971).

regions. First of all, by definition, the electrons in this region are of extended states (since they are not in the gap), therefore diffusion can take place even at $T = 0°K$. By using Einstein's relation,

$$\mu = \frac{e\,D}{kT} \tag{2.14}$$

where D is the diffusion constant, the product μT is finite even at $T = 0°K$. Secondly, there is a limitation for the electrons to behave as free carriers and propagate with occasional scattering as in crystalline semiconductors. This limitation has been emphasized in section 2.1 that the mean free path λ cannot be less than the interatomic separation. If we assume the average interatomic distance a to be about 3 $\mathring{A}$, the mean free path for a wave-like electron should not be less than this. The corresponding mobility is about 5 cm^2/V sec. Hence for a mobility lower than 5 cm^2/V sec, it is not possible to assume a wave-like propagation mechanism since the mobility is too low for the mean free path to be as large as the interatomic separation.

Cohen has suggested that in the mobility region from 5 cm^2/V sec to about 10^{-2} cm^2/V sec (mobility shoulder), the electrons can be treated as Brownian particles, which have an irreversible motion resulting from the random, fluctuating forces exerted by the fluctuating atoms or molecules on the Brownian particles. The motion of Brownian particles is diffusive, and has a finite value at absolute zero; it depends mainly on the fluctuation of the system. Since the electrons in this region are of extended states, the fluctuating forces can easily give sufficient energy to the electrons to overcome the energy barriers between sites and to jump from site to site.

The diffusion coefficient D for the Brownian motion can be expressed in its most primitive form (the expression of D can be seen in most statistical mechanics texts; for example, Pathria, "Statistical Mechanics" 1973),

$$D = \frac{1}{6} d^2 \nu_{e\ell}, \tag{2.15}$$

where d is the average distance for one jump, which is equal to the interatomic separation a; and $\nu_{e\ell}$ is the mean frequency of jumping out of a site. From equations (2.14) and (2.15) the mobility can be expressed as

$$\mu = \frac{1}{6} \frac{ea^2}{kT} \nu_{e\ell} \tag{2.16}$$

he magnitude of $\nu_{e\ell}$ is approximately equal to the crystalline electronic frequency (may be slightly lower due to the fluctuations), which can be written as

$$\nu_{e\ell} = \frac{h}{m^* a^2} \tag{2.17}$$

$\nu_{e\ell}$ is then of the order of 10^{15} sec^{-1}. Thus equation (2.16) can also be written as

$$\mu = \frac{e\, h}{m^*\, kT} \tag{2.18}$$

The mobility of electrons in the mobility gap and also in mobility shoulder has already been discussed. For electrons with energies $(E - E_c) >> kT$, the mean free path is larger than the interatomic separation, and hence electrons have wave-like characteristics and therefore can be transported via propagation with occasional scattering mechanism. They can be regarded as free electrons having well defined effective mass and wave-vector $\bar{K}$. The mobility in this region would have the same form as

that in crystalline solids, or,

$$\mu = \frac{e\tau}{m^*} \qquad (2.19)$$

This expression is also valid for holes but with energies $(E_v - E) << kT$.

According to equations (2.18) and (2.19) and previous discussions, it is possible to draw a rough scale for the mobility shown in Fig. 2.9, and also the corresponding mobility region in N(E) distribution shown in Fig. 2.10.

As a summary, it may be good to quote the interpretation of Fig. 2.9 from Cohen (1970), who stated: "The regimes of propagation with occasional scattering ranges from about 10^8 cm^2/V sec down to about 5 cm^2/Vsec when the Brownian motion regime sets in. The carrier states remain extended down to mobilities of order 10^{-2} cm^2/V sec when the states become localized and the phonon-assisted hopping takes over. These borderline values of 5 cm^2/V sec and 10^{-2} cm^2/V sec are only rough estimated and depend on the family of materials under study".

2.6. The Mott-CFO model

Cohen, Fritzsche and Ovshinsky (1969) have proposed a simple band model for amorphous semiconducting covalent alloys. A similar model has also been worked out by Mott (1968). This model has been supported by most of the experimental results except the anormalous Hall effect. The most successful part of this model is that it establishes a mobility structure instead of an energy structure; through which most of the characteristics in amorphous semiconductors can be easily understood. The important features of this model discussed in the previous sections are now summarized below:

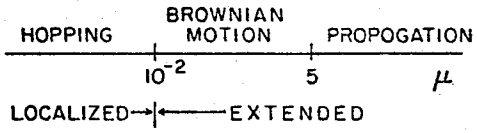

Fig. 2.9. The mobility (μ) scale showing the phonon assisted hopping, Brownian motion, and propagation regimes. The units are cm^2/V sec for μ. (After Cohen, 1970).

1. All valence bonds are saturated. The individual atoms of amorphous alloys have their valence requirements locally satisfied; i.e., the widely varying valences are saturated and behave as intrinsic materials.
2. There exist two well defined energies E_c and E_v, at which the carriers change their mobility abruptly from normal value to an extremely small value. The energies E_c and E_v associated with the mobility rather than with the density of states, and thus they are called the mobility gap edges.
3. The carriers with energies below E_v and those with energies above E_c are of extended states.
4. Both bands of extended states have tails of localized states. The carriers in these states are trapped and localized. These tail states are distributed in the mobility gap.
5. The increase the degree of disorder will consequently increase the number of the possible energy state, and thus increase the number of the localized state. The band tails are therefore to extend more deeply into the gap. In amorphous semiconducting covalent alloys, the disorder is sufficiently large so that the tail states extending from E_c and E_v overlap.
6. A localized state can always be identified as a valence-localized state or conduction-localized state. That is, the localized states in the conduction band tail have the electronic characteristics and those in valence band tail have the hole characteristics. The charge characteristics of any localized states can always be identified as hole or electronic.

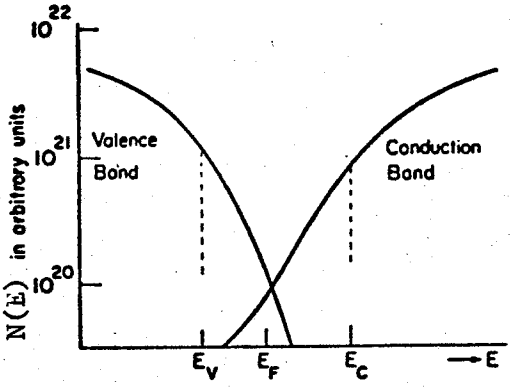

Fig. 2.11. The density of states as a function of electron energy. E_v and E_c are the energies of the mobility edges. States which are neutral when occupied are associated with the valence band, and the states which are neutral when empty are associated with the conduction band; these two bands cross the mobility gap. (After Cohen, 1970).

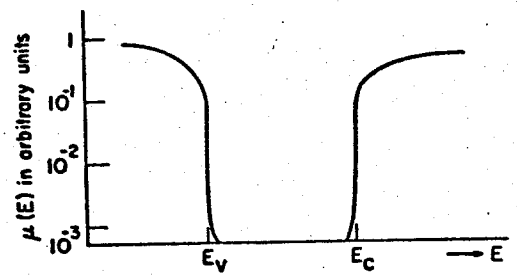

Fig. 2.12. The electron and hole mobilities as functions of electron energy. (After Cohen, 1970).

7. There is a distribution of charge traps in the middle region of the mobility gap. Since the valence tail states are locally neutral when occupied, therefore an empty valence tail states contributes to a positive trap. Similarly, an occupied conduction tail state contributes to a negative trap. At $T = 0°K$, the valence tail states are empty above E_F and the conduction tail states below E_F are occupied; these states form a distribution of charge traps around E_F.
8. The transport processes change their character from extended states to localized states at the transition energy levels E_c and E_v. Between E_c and E_v, the localized carriers may move by phonon-assisted hopping amongst the localized states. With energies several kT above E_c and below E_v, the carriers can be considered as free carriers, the conduction mechanism for these carriers is of "in-band" conduction and very similar to the intrinsic conduction in crystalline semiconductors. The carriers with energies just above E_c and just below E_v can be considered as Brownian particles, the conduction of these carriers is of diffusion type.

The features of the Mott-CFO model are shown schematically in Fig. 2.11 and Fig. 2.12.

PART 2. DC CONDUCTIVITY AND TRANSPORT MECHANISMS

The earliest experimental studies on chalcogenide glasses probably be the work of Uphoff and Healy around 1960. However, the electronic properties of these materials did not draw much attention from the research

of solid state devices and physics until 1964. After 1966, the success in developing switching and memory devices with amorphous semiconductors by Ovshinsky had dramatically prompted investigations into the problems of transport mechanisms in chalcogenides. Many experimentalists, theoreticians and development engineers have been attracted to this area primarily because of the high potential of these materials for electronic devices. In 1969, one of the most important symposium was held in New York (SEAS Symposium, New York City, May 14-17, 1969), and the subjects of this symposium have stimulated the development of most recent work.

In the past few years, the transport properties of chalcogenide glasses have been extensively studied, but the transport mechanisms are still not very clear. The discussion in Part 2 is based mainly on the Mott-CFO model though it is somewhat speculative, because it is generally agreed with experimental results. Also, it is necessary to emphasize that the discussion in this Part and Part 3 is constrained to only the chalcogenides, which have a pseudogap structure so that the Mott-CFO model can be applied.

2.7. The temperature dependence of dc conductivity

The Ovonic glasses (e.g. Ge-Si-As-Te system) have switching characteristics at high fields (10^6 V/m and up at 300°K), most of the temperature-dependent dc conductivity measurements are performed in the low field (ohmic) region. Moreover, since the temperature dependence of dc conductivity of chalcogenide glasses has a completely different characteristic at low temperaturesfrom that at high temperatures, it is therefore convenient to discuss them separately as follows:

(A) Temperature dependence of dc conductivity at high temperatures

The temperature-dependent dc conductivity of chalcogenide glasses

at high temperatures (200°K to 500°K) has been observed in numerous experiments to follow the exponential relation:

$$\sigma = \sigma_o \exp(-\Delta E_o/kT) \tag{2.20}$$

where σ: dc conductivity ($ohm^{-1}\ cm^{-1}$)

σ_o: an empirical coefficient ($ohm^{-1}\ cm^{-1}$)

ΔE_o: electrical activation energy (eV)

k: Boltzmann constant (eV/K°)

T: temperature (K° from about 200°K to 500°K)

Equation (2.20) holds in a considerable wide temperature range, also the electrical activation energy ΔE_o is comparatively stable in this temperature range. To understand the physical implications of this equation, a number of experiments have been done by comparing the conductivity of amorphous Ge film with that of the crystalline Ge. (Clark 1967; Grigorovici et al. 1966; Walley and Jonscher 1968; Chopra and Bahl 1970; Stuke 1970). The values for ΔE_o for amorphous Ge so far reported are quite scattering, and vary from 0.15 eV to 0.55 eV at 300°K. This may be due to different sample preparation processes, different film thicknesses, and possibly different amounts of annealing applied to the sample. Despite of the differences, it is reasonable to say that the activation energy of amorphous Ge film is comparable to that of crystalline Ge (about 0.40 eV at 300°K).

The activation energy ΔE_o for chalcogenide glasses so far reported are quite consistent, probably because chalcogenides are not so easy to

be recrystallized through normal heat treatment. It is generally accepted that ΔE_o in chalcogenides is larger by about 10 to 20% than half of the optical band gap. The typical temperature-dependent dc conductivities of some chalcogenides are shown in Fig. 2.13.

(B) Temperature dependence of dc conductivity at low temperatures

conductivity for chalcogenide glasses at low temperatures (say, 150°K and down) is very difficult to measure. The dc conductivity of Ge-Si-As-Te system at 150°K has been measured by Male (1970), and by Marshall and Miller (1973), which is of the order of 10^{-14} ohm^{-1} cm^{-1} when subjected to an applied field 10^5 V/m. On the other hand, it is not suitable to apply a high field for two reasons. Since the dc conductivity is of field dependent (Marshall and Miller 1973), the applied field must be kept constant within the whole temperature range interested; also Joule heating process would occur in high temperature region (at about 10^6 V/m at 300°K, 10^5 V/m at 420°K). Moreover, to apply a high field (say higher than 10^9 V/m) to the sample at very low temperatures (lower than 77°K), serious noise problem would easily induce at the electrodes which is technically difficult to handle. At the present time, there is no dc conductivity reported in literature for Ge-Si-As-Te system at temperature lower than 150°K. The extremely low temperature characteristics of these materials can only be conjectured through other amorphous materials which have lower resistivities. Elemental amorphous germaniumum has been commonly used for this purpose ; not only because the resistivity of Ge film (about 10^{11} ohm cm at 25°K, Clark, 1967) is much smaller compared with the chalcogenides at low temperatures, but also the transport mechanisms for elemental materials are much easier to understand than that

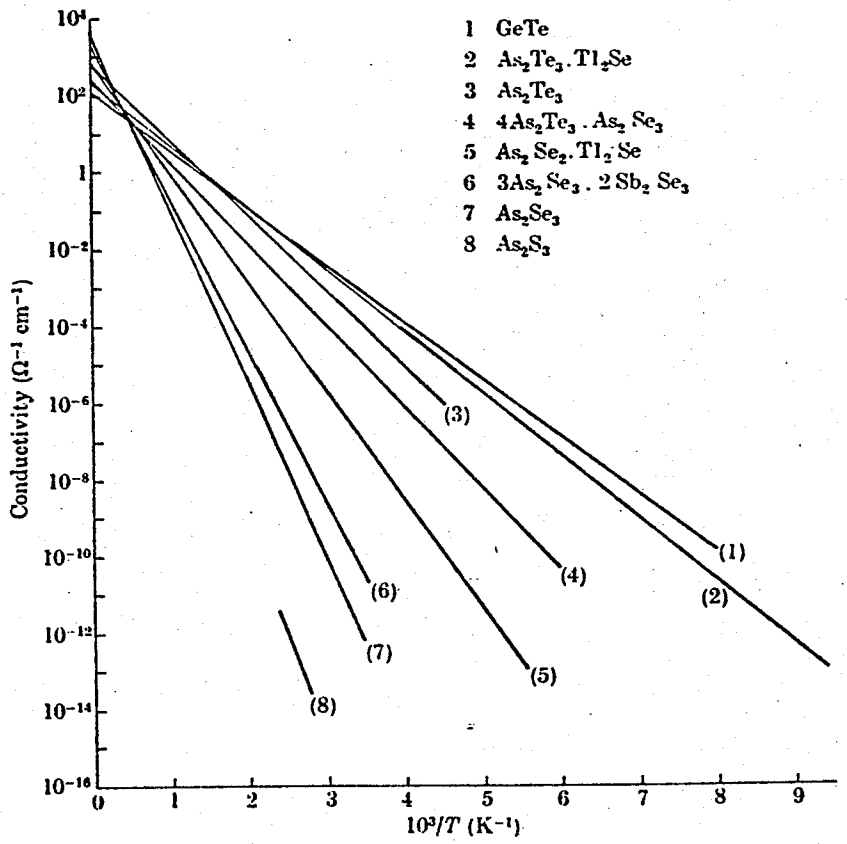

Fig. 2.13. Temperature dependence of electrical conductivity in some amorphous chalcogenide semiconductors, illustrating the relationship $\sigma=\sigma_o \exp(-\Delta E/kT)$. Heavy lines are the experimental results and fine lines are the extrapolation of $1/T = 0$ (note that the actual variation of σ with T is not expected to follow this extrapolation). (After Mott and Davis, 1971).

of the compounds.

Clark (1967) has reported that in the temperature range from about 200°K to 25°K, the conductivity of amorphous Ge film follows the relation of $\ln \sigma \propto T^{-1/4}$, which in fact, has been proposed by Mott based on a phonon-assisted hopping mechanism. Fig. 2.14a and b shows Clark's data plotted in log ρ against T^{-1} and $T^{-1/4}$. We can see that the linearity of log ρ versus $T^{-1/4}$ extends to relatively high temperatures (at least exceed 200°K at which $T^{-1/4} = 0.27$). The wide extended temperature range for the validity of $T^{-1/4}$ relation is totally unexpected in Mott's model. It seems not convincing that the phonon-assisted mechanism dominates the conduction at such relatively high temperatures. Furthermore, Cohen (1970) argued that in Mott's model the electrons are assumed hopping over a random distribution of localized states without interacting to each other. This can be valid only when the temperatures are so low that the electron correlation can be ignored. Particularly for highly disordered materials as chalcogenides, the density of localized electrons is so high (in the order of 10^{19} cm^{-3} eV^{-1}), the average distance between these electrons becomes very small (about 25 Å); the electron-electron interaction energy is of the order of 0.1 eV, which is comparable with the mean activation for hopping and therefore would eliminate the possibility of $T^{-1/4}$ law.

Several other investigators (for example, Walley and Jonscher 1968, in temperature range 55°K to 300°K) have confirmed that the log σ versus $T^{-1/4}$ relation at low temperatures. The $T^{-1/4}$ relation has been generally accepted (at least in very low temperature region, say, 150°K and down). On the other hand, it should be noted that the experimental results showing the $T^{-1/4}$ relation interpreted by the linearity of the plot with

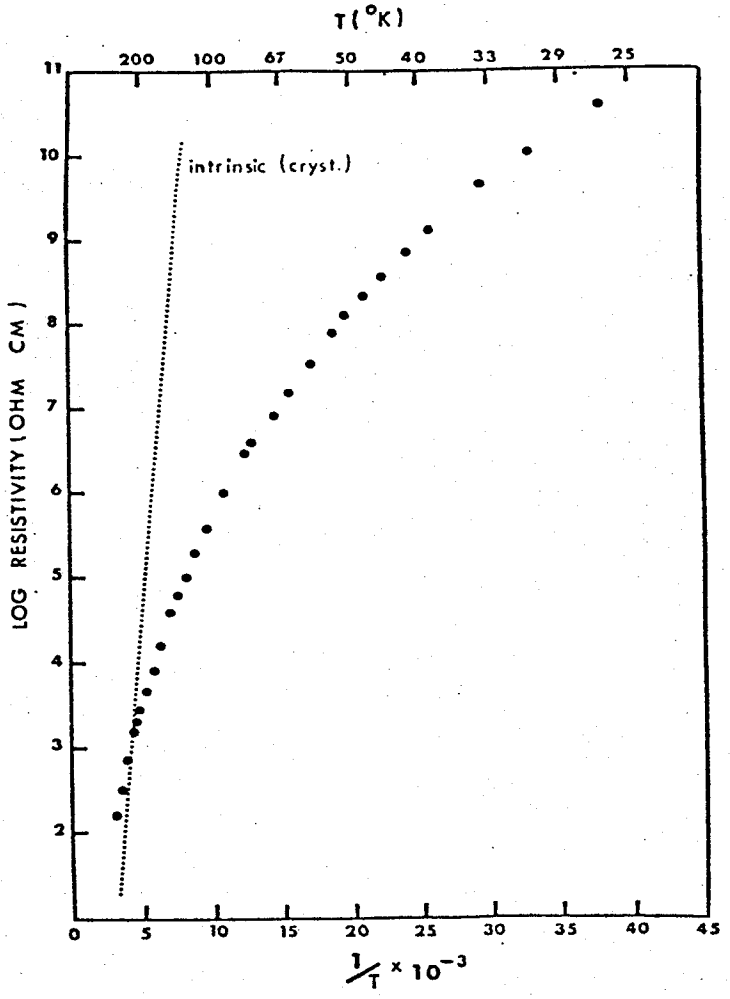

Fig. 2.14a Temperature dependence of resistivity of amorphous germanium. (After Davis and Shaw, 1970).

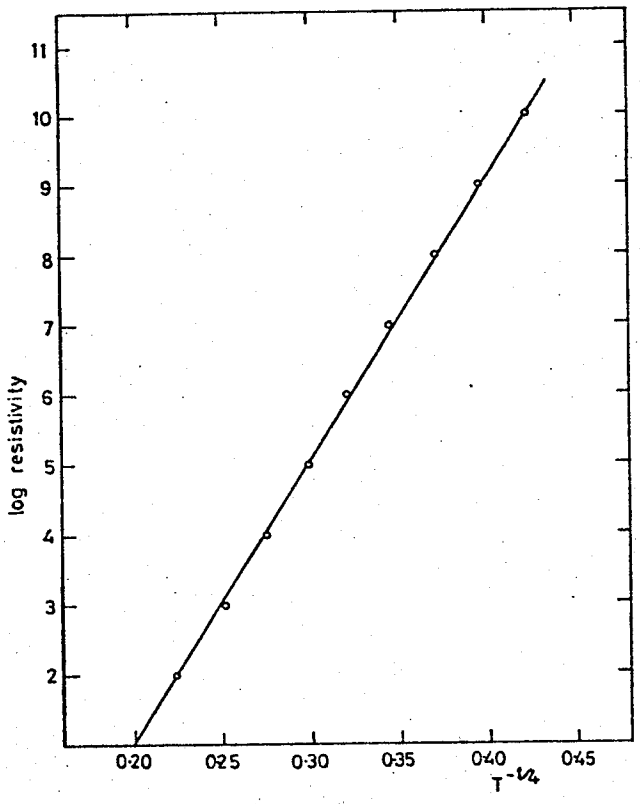

Fig. 2.14b Temperarature dependence of resistivity of amorphous germanium replotted as log resistivity versus $T^{-\frac{1}{4}}$. (After Davis and Shaw, 1970).

$\ell n\ \sigma$ versus $T^{-\frac{1}{4}}$ is not sufficient to identify a conduction mechanism. To show the ambiguity which can be introduced by the plots, Hill (1971), has plotted σ as a function of $T^{-\frac{1}{4}}$, $T^{-1/7}$ and $T^{-1/3}$, with T in the range 20°K to 300°K, and found that over most of this range, the graphs are mostly indistinguishable except at extremely low temperatures is there a significant deviation, as shown in Fig. 2.15.

Some basic properties of $Ge_{10}\ Si_{12}\ As_{30}\ Te_{48}$ are listed in Table 1.

2.8. "In-band" conduction mechanism

The temperature dependence of dc conductivity at high temperatures (250°K to 500°K) follows an exponential form shown in equation (2.20), and very similar to the band conduction in crystalline semiconductors. It is therefore reasonable to associate the conduction mechanism in this temperature range with "in-band" conduction mechanism. What we mean by "in-band" conduction is that the conductivity is mostly contributed by the carriers with energies other than the mobility gap $E_v < E < E_c$. The carriers are extended rather than localized, and have wave-like properties (wave vector $\bar{K}$ and thus effective mass m_n^* and m_p^* can be well defined) which are similar to the free carriers in crystalline solids. Diffusive and hopping type conduction of course would occur in mobility shoulder and mobility gap region respectively; but they are too small compared with the conduction involving a wave-like propagation with occasional scattering.

The necessary condition for wave-like propagating conduction to occur is that the mean free path λ of the carriers must be larger than the De Broglie wave-length of the electron (or alternatively, λ must be larger than the interatomic separation). This could happen only when

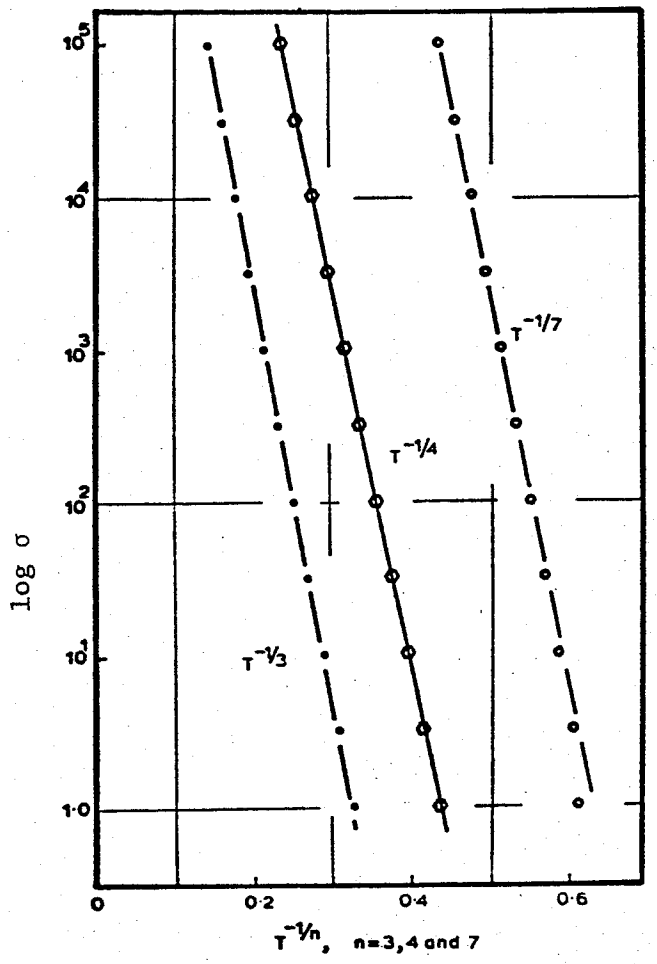

Fig. 2.15. The plot of log σ versus $T^{-1/n}$ in the temperature range 20 to 300°K. (After Hill, 1971).

Table 1. Some experimental data of Ge_{10} Si_{12} As_{30} Te_{48}

Properties	Empirical values
ΔE_{opt}	---
ΔE_o	0.55 to 0.5 eV (500°K to 150°K)
ΔE_s	---
σ	4.05×10^{-8} ohm^{-1} cm^{-1} (298°K)
σ_o	1.92×10^{4} ohm^{-1} cm^{-1}
$N_{(E_F)}$	2×10^{19} cm^{-3} eV^{-1} (300°K)
T_o	598°K
η	3.1 (thickness ~ 5μm)

where ΔE_{opt}, ΔE_o and ΔE_s are the optical band gap, electrical and TEP activation energies, respectively. T_o is the softening temperature and η is the refractive index.

the temperature is high enough to activate significant concentration of carriers to the energy region beyond the mobility gap. The electrical activation energy ΔE_o for Ovonic glasses obtained from dc conductivity measurement is about 0.55 eV which is about the same order of the optical band gap ΔE_{opt}. The consistence of electrical and optical band gap reinforce the possibility that "in band" carriers dominate the conduction at high temperatures. We shall follow this assumption to develop a tentative model using a practical approach more or less similar to that for intrinsic crystalline semiconductors. This model, of course, is not necessary true, since it involves a number of assumptions which are not easy to be justified experimentally. However, we shall specify these assumptions, and discuss the physical implications behind them.

First of all it is desirable to outline the experimental evidences as follows:

(i) The density of localized states near E_F in the band gap can be estimated by both electrical and optical measurements. Thermostimulated current measurements and field effect experiments indicate that $N(E_F)$ of the order of 10^{19} cm^{-3} eV^{-1}, however, optical absorption data give an upper limit for $N(E_F)$ in the order of 10^{16} cm^{-3} eV^{-1}. The conflict between these measurements has been analyzed by Fritzsche (1971). Since most of the chalcogenides are not sensitive to doping (usually no anomality observed with doping density up to 10^{19} cm^{-3}), it is reasonable to assume that the density of localized states at E_F is as high as 10^{19} cm^{-3} to make the self-compansation possible.

(ii) Temperature-dependent conductivity follows an exponential form, with the electrical activation energy ΔE_o about 0.1 to 0.3 eV larger

than half of the optical band gap.

(iii) The pre-exponential factor is about the same for most chalcogenides despite of chemical compositions; and have values from 10^2 to 10^4 ohm^{-1} cm^{-1}.

(iv) Thermoelectric power measurements from chalcogenides normally show that hole carriers are dominant.

(v) Measurements of electrons tunneling from a metal through an oxide barrier layer into an amorphous semiconductor show that E_F remains near the gap center in the temperature region from 300°K to 78°K. (Osmum and Fritzsche 1969).

Making use of the above evidences, we can conjecture a conduction model through appropriate explanations of the electrical activation energy ΔE_o and the Fermi level E_F in chalcogenides.

(A) Electrical activation energy

Electrical activation energy ΔE_o is defined empirically by the exponential form of temperature-dependent conductivity given in equation (2.20). The electrical activation energy is generally a temperature dependent quantity and is expected to have an zero slope at $T = 0°K$. As the temperature increases, the activation energy is expected to decrease because of the increase number of phonon It decreases nonlinearly with increasing T until T reaches the Debye temperature. Above Debye temperature, the activation energy becomes linear with the changing temperature and can be approximated by the relationship (Fritzsche 1971),

$$\Delta E(T) = \Delta E_o - \beta T \qquad (2.21)$$

where ΔE_o is the intercept of $\Delta E(T)$ by extrapolating equations (2.20) from some higher temperature to $T = 0°K$. From Fig. 2.16, it is easily

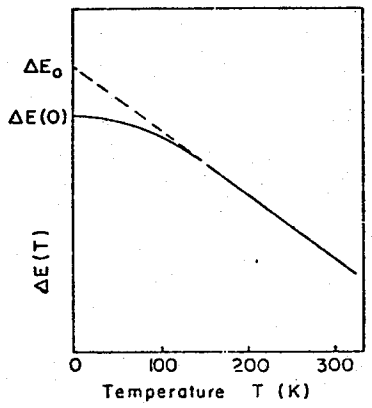

Fig. 2.16. The expected temperature dependence of $\Delta E = E_F - E_v$ or of $E_c - E_F$. The slope of an Arrhenius plot of the conductivity gives ΔE_o and not $\Delta E(o)$. (After Fritzsche, 1971).

seen that ΔE_o in general must be higher than the activation energy at $T = 0$ which is represented by $\Delta E(o)$.

By substituting equation (2.21) to equation (2.20), we have,

$$\sigma(T) = \sigma_o \exp(\beta/k) \exp(-\Delta E_o/kT) ,$$

or

$$\sigma = \sigma_o' \exp(-\Delta E_o/kT). \qquad (2.22)$$

The temperature factor β contributes to a constant prefactor to the exponential of equation (2.20). In fact, equation (2.22) is the actual form which has been observed experimentally. The plot of $\ell n\, \sigma$ versus T^{-1} gives ΔE_o. Apparently, the quantity ΔE_o bears no direct physical meaning related to the band gap unless the conduction can be interpreted as totally intrinsic band to band conduction as in intrinsic crystalline semiconductors.

The quantity ΔE_o observed is usually interpreted as $E_F - E_v$ (or $E_c - E_F$ in n-type conduction). Assuming intrinsic band to band conduction, E_F is at the middle of the gap,

$$\Delta E_o = E_F - E_v = \frac{1}{2} E_g. \qquad (2.23)$$

This is of course not necessarily true; since all the experimental results are in favour of unipolar conduction, either holes or electrons dominant conduction. Fritzsche (1970, 1971) has suggested that ΔE_o may not be the amount of energy equals to $E_F - E_v$ since ΔE_o is only the extrapolation of the activation energy at $T = 0°K$, but not $\Delta E(o)$, and it bears no direct relationship with the band gap. Also, since it is of unipolar conduction, either $n > p$ or $p > n$, it is unlikely that E_F can be assumed to be located at the middle of the gap. The argument on

ΔE_o has not yet been settled at the present stage. However, by assuming $\Delta E_o = \frac{1}{2} E_g$, we are able to estimate the free carrier concentration and also the mobility ratio, which are quite consistent with the experimental result (Böer 1969). To understand the electrical activation energy ΔE_o, a detail discussion on Fermi level would be helpful.

(B) The Fermi energy in amorphous covalent alloys

Fermi energy E_F is one of the most important concept crystalline semiconductor theory. In the case of intrinsic crystalline semiconductor, free carrier densities n and p are directly related to the location of E_F in the band gap. For doped semiconductor, if impurity density is of several order higher than the intrinsic carrier density n_i, the Fermi energy is determined by the density of ionized impurities. In amorphous semiconducting covalent alloys, the localized state density usually is high (10^{19} to 10^{20} cm^{-3} eV^{-1}) compared with the free carrier density (less than 10^{11} cm^{-3}); the Fermi energy should be determined solely by the density of localized states to fulfill the charge neutrality requirement. By definition of Fermi energy, the probability for an energy state above E_F to be occupied must equal to the probability of the energy state with the same energy distance below E_F to be emptied. Therefore, E_F can be determined by the charge neutrality condition:

$$n + \sum_j {}^jN_a = p + \sum_i {}^iP_d \qquad (2.24)$$

where ${}^jN_a$ is the density of occupied conduction tail states at energy E_j, ie, the density of trapped electrons at E_j. And ${}^iP_d$ is the density of empty valence tail states at energy E_i, i.e., the density of trapped holes at E_i.

Since n and p are very small compared with $\Sigma_j {}^{j}N_a$ and $\Sigma_i {}^{i}P_d$ respectively, E_F can be determined by the equation:

$$\Sigma_j {}^{j}N_a = \Sigma_i {}^{i}P_d \qquad (2.25)$$

The location of E_F in the band gap depends on the energy distribution of the trapped electron density N_a and trapped hole density P_d. E_F can be assumed in the middle of the mobility gap if and only if the energy distribution of the trapped electron density and trapped hole density is symmetrical with respect to E_F. Theoretically, there is no implication from the theory to support this symmetrical distribution; nor there is experimental evidence to show directly this property. However, by assuming simple intrinsic crystalline conduction, the measurements of electron tunneling in a metal-oxide-amorphous system show that E_F is near the gap center as reported by Cohen, Fritzsche and Ovshinsky (1969). It is therefore generally accepted that E_F is located at the middle of the gap. This is, of course, very speculative, since there is no experiment as yet which can directly measure the mobility gap. Optical absorption measurement may have been one of the generally accepted experiments employed for the determination of E_g. However, there appears a tail region at lower photo energies in the plot $(\alpha\, h\, \nu)^{\frac{1}{2}}$ versus $h\nu$, the optical band gap can only be obtained by extrapolating the linear portion of the curve to $\alpha = o$ (Fig. 2.17). This will give some degree of uncertainity to the value of ΔE_{opt}. Another important problem is that the interpretation of optical absorption coefficient leads to a conclusion that the density of localized states in the gap is about 10^{16} cm^{-3} eV^{-1} (Fritzsche 1971), which is too small to explain the self-compensation of doping impurities up to 1%, and also other electrical properties. We must admit that at

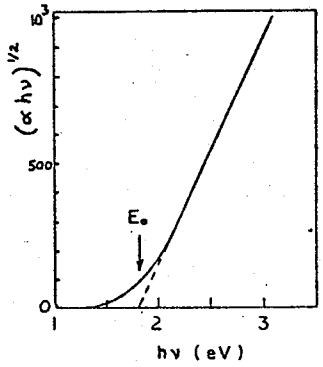

Fig. 2.17 Dependence of $(\alpha\ h\ \nu)^{\frac{1}{2}}$ on photon energy for amorphous $As_2\ Se_3$. The intercept of the straight line portion with the abscissa defines the optical gap ΔE_{opt}. (After Frtizsche, 1971).

this stage, the measurement of the real band gap of amorphous covalent alloys is very difficult to achieve, the activation energy ΔE_o as well as ΔE_{opt} may bear some relations to the real band gap, but not necessary a simple one as in equation (2.23).

(C) Intrinsic approximation

Roosbrveck and Casey (1972) have proposed that the Fermi level of amorphous semiconductors with high resistivities is pinned up in a way to make the dc conductivity minimum and near intrinsic. Although theoretically it is not easy to locate the exact position of the Fermi energy in the band gap, it is commonly accepted that by assuming an intrinsic conduction and let $E_F = \frac{1}{2} E_g$, we can explain very well the experimental results. In fact, the free carriers at high temperatures have wave-like characteristics, therefore the transport process would not be very much different from crystalline semiconductors. By assuming intrinsic conduction it is not necessary to assume $n = p$ as a consequence of $E_F = \frac{1}{2} (E_c + E_v)$, since the effective mass may not be the same for holes and electrons. Böer (1969) have suggested an intrinsic model for amorphous covalent alloys in which the Fermi level is assume to locate exactly at the middle of the mobility gap; the conduction is therefore ambipolar and both n and p are significantly contributed to conductivity. The only thing in Boer's model different from intrinsic crystalline semiconductors is that the band edges of chalcogenides are perturbated as a result of high degree disorders. The perturbation of band edges can be estimated approximately to be of $(\Delta E_o - \frac{1}{2} \Delta E_{opt})$; i.e., the difference between electrical activation energy and half the optical band gap. This amount of energy is treated as potential barrier just inside the band edges so that the major conduction takes place inside the band edges rather than at the

band edges.

Since Böer's model viewed from perturbation of band edges and from the approximation of intrinsic conduction, which is quite different from the theory presented in Part 1, it is necessary to redefine some of the terms to avoid confusion. Boer has assumed that the optical band gap from optical absorption measurement refers directly to the real band gap E_g; with E_c and E_v corresponding to the optical band edges. The electrical activation energy obtained from temperature-dependent conductivity measurement does not physically correspond to the band gap, it refers only to the energy of the "effective level", at which the major conduction takes place. Thus, we have,

$$\Delta E_o = \frac{E_g}{2} + \varepsilon \tag{2.26}$$

where ε is the effective potential barrier as a result of disorder. For an ambipolar conduction, we have,

$$\sigma = \sigma_n + \sigma_p = \sigma_o \exp(-\Delta E_o/kT) \tag{2.27}$$

where

$$\sigma_o = \sigma_{on} + \sigma_{op}; \tag{2.28}$$

σ_{on} and σ_{op} are the extrapolation of conductivities at $T = 0°K$ contributed by n and p. Also;

$$\sigma_{on} = e\,\mu_n\,N_c(\varepsilon) \tag{2.29a}$$

$$\sigma_{op} = e\,\mu_p\,N_v(\varepsilon) \tag{2.29b}$$

where $N_c(\varepsilon)$ and $N_v(\varepsilon)$ are the effective energy state densities at the

conduction and valence levels respectively. Since the potential barrier ε is of the order of 0.1 eV (only a small portion of the band width E_g), in good approximation, the effective level density can be expressed as (Spenke 1958):

$$N_{c,v}(\varepsilon) = N_{c,v} \frac{4}{\sqrt{\pi}} \left(\frac{\varepsilon}{kT}\right)^{\frac{1}{2}} \tag{2.30}$$

with

$$N_{c,v} = 2\left(\frac{m^*_{n,p}\, kT}{2\pi \hbar^2}\right)^{3/2} \tag{2.31}$$

$N_{c,v}$ is the level density at conduction band edge or valence band edge, respectively.

In equation (2.26), an assumption $E_F = \frac{E_c + E_v}{2}$ has been made. However, it does not mean that the intrinsic hole and electron densities are equal; since E_F is determined by the trap distribution rather than by the free carrier densities. By assuming intrinsic conduction, it is obvious that n and p can be different if the effective massess m^*_n and m^*_p are different. Since the free carriers at high temperatures have wave-like characteristics, the effective masses associated with them are more or less well defined. However, the $E - K$ relationship of hole and electrons in disordered media have not yet been developed, it is not possible to find the magnitude of m^*_n and m^*_p. Böer (1969) has suggested that the effective masses m^*_n and m^*_p can be related if we can assume a simple band structure. Under simple band consideration, the effective mass is inversely proportional to the curvature of the $E - k$ curve, and the curvature of the curve is a function of the band width of the conduction and valence bands. Thus, we have

$$\frac{m_p^*}{m_n^*} \alpha \frac{\Delta E_c}{\Delta E_v} \tag{2.32}$$

where ΔE_c and ΔE_v are the widths of the conduction and valence bands, respectively. Apparently, ΔE_c must be larger than ΔE_v since the conduction band is split by the outmost energy level of the atoms whereas the valence band is of one level down. So we have,

$$\frac{m_p^*}{m_n^*} = M_r > 1 \tag{2.33}$$

The magnitude of the effective mass ratio M_r cannot be deducted from the theory; instead, we can assume a value for M_r to compare with the experimental results. By means of M_r, we can estimate the p/n ratio, the μ_p/μ_n ratio, and the ratio of conductivities σ_n/σ_p.

1. The p/n ratio.

Substituting equation (2.33) to equation (2.31), we obtain

$$\frac{N_v}{N_c} = \left(\frac{m_p^*}{m_n^*}\right)^{3/2} = M_r^{3/2}. \tag{2.34}$$

Putting this in equation (2.30), we have

$$\frac{N_v(\varepsilon)}{N_c(\varepsilon)} = M_r^{3/2} \tag{2.35}$$

Since $E_F = \frac{E_c + E_v}{2}$, we have

$$E_F - E_v = E_c - E_F = \Delta E_o \tag{2.36}$$

Therefore,

$$(n,p) = N_{c,v}(\varepsilon) \exp(-\Delta E_o/kT) \tag{2.37}$$

and

$$\frac{p}{n} = \frac{N_v(\varepsilon)}{N_c(\varepsilon)} = M_r^{3/2} \tag{2.38}$$

2. The

Recalling equation (2.19) in section 2.5, the mobility at high termperatures is:

$$\mu = \frac{e\,\tau}{m^*} = \frac{e\lambda}{\sqrt{3kT\ m^*}} \tag{2.39}$$

where τ is the average relaxation time between two scattering of the free carriers. Assuming the mean free path is the same for both electrons and holes (since on the basis of the assumption $E_F = \frac{E_g}{2}$, the density of traps for electrons is equal to that for holes and are symmetical with respect to E_F), we have,

$$\frac{\mu_n}{\mu_p} = \left(\frac{m_p^*}{m_n^*}\right)^{\frac{1}{2}} = M_r^{\frac{1}{2}} \tag{2.40}$$

3. The ratio of conductivities σ_n/σ_p

From equations (2.29), (2.35) and (2.40), we have,

$$\frac{\sigma_{op}}{\sigma_{on}} = \frac{\mu_p}{\mu_n}\,\frac{N_v(\varepsilon)}{N_c(\varepsilon)} = M_r^{-\frac{1}{2}}\,M_r^{3/2} = M_r, \tag{2.41}$$

and from equations (2.27), (2.28), and (2.41) we obtain

$$\frac{\sigma_p}{\sigma_n} = \frac{\sigma_{op}}{\sigma_{on}} = M_r \tag{2.42}$$

Equation (2.42) reveals a very important feature of highly disordered intrinsic semiconductors that the conduction should be of p-type if the conduction follows the assumptions of the simple band intrinsic approximation.

There are, in fact, quite a number of problems involved in Böer's

model. For instance, the Fermi level is not necessary exactly at the middle of the band gap; also the effective mass ratio may not be inversely proportional to the width of the bands since the conduction normally takes place at the bottom but not at every energy state of the bands. Therefore, this model can only be used as an approximation band on intrinsic, a bipolar and simple-band assumptions. As long as there is no quantitative evaluation available for the p/n ratio, mobility ratio and the ratio of conductivities, it is most instructive to compare the results of the analysis of a naive band model as such with those of the experiment obtained on chalcogenide glasses.

2.9. The phonon-assisted hopping conduction mechanism

The dc conductivity of amorphous Ge films at low temperatures follows the well-known relation of $\ln \sigma \propto T^{-\frac{1}{4}}$ as suggested by Mott(c.f. section 2.7(B)). This relation is based on a simple hopping conduction model which is developed mainly for the conduction at very low temperatures. The phonon energy at these low temperatures is so small that the number of electrons excited from levels below E_F to the conduction band is too little to give significant contribution to the conductivity. The conductivity under this condition becomes very small, and the conduction would be dominated by the hopping of electrons amongst localized states with energy near E_F.

As mentioned in section 2.7(B), the $T^{-\frac{1}{4}}$ law has been observed by Clark and Walley in the temperature range from 30°K up to 250°K. Some investigators (for instance, Hill 1971) believe that the phonon-assisted hopping may be the dominated conduction up to 300°K. Unfortunately, the model suggested by Mott is very much simplified, in which the electron-electron interaction, the in band carrier contribution, and the difference

between the density of states and the occupied state density have not been considered. These factors became very important at higher temperatures. It seems not reasonable to estimate the actual contribution of hopping at higher temperatures by using this model. It is most likely that in amorphous Ge films, phonon-assisted hopping dominates the conduction only at low temperatures (150°K and down); at higher temperatures (say 150°K to 250°K), the conduction may be contributed significantly by hopping as well as "in band" conduction. In this section, only the conduction at temperatures lower than 150°K are considered, so that the following basic assumptions can be made:

1. The electron-electron interaction at these low temperatures can be completely ignored.
2. At these low temperatures, only those electrons with energies within the range of order kT at the Fermi level need be considered as taking part in the conduction process. Those with lower energies will on the average have not enough energy to jump to an energy state above E_F.
3. According to the selection rule introduced by Mott (1968), the electrons will prefer to jump to a further distance to the lower energy state, despite of the overlap of orbital is small. For two localized states, the larger the separation in space, the smaller is the overlap of orbitals between these two states and hence the probability for hopping is smaller. On the other hand, the further an electron can tunnel, the more states it can choose and hence the greater the chance for it to find an empty state with lower energy to jump into; therefore the probability for hopping is greater. Mott has conjectured that at low temperature,

the total energy of electron is too small to overcome the potential barrier between the states and therefore the maximum hopping conduction occurs under the condition that the energy region for hopping conduction to take place is of minimum with of the order of kT with maximum average hopping distance.

Under these 3 assumptions, the hopping model can only be valid at very low temperatures at which the electron-electron interaction, and also the electrons with energies much lower than E_F can be completely ignored.

(A) The $T^{-\frac{1}{4}}$ law for hopping conduction

There are 3 basic factors which can be used to characterize the hopping motion of an electron jumping from one localized state to another with higher energy:

(i) The Boltzmann factor, in the form of $\exp(-W/kT)$

This factor characterizes the energy difference between two states (denoted by W) involving the jump and the thermal energy of the electron (kT).

(ii) The electronic frequency ν_{ph} for an electron to jump between sites

This factor is very complicated, it depends on the phonon spectrum of the material and also temperature. Assuming ω_{max} is the maximum phonon frequency, and the electronic frequency for hopping is $\nu_{ph} = \frac{W}{\hbar}$. Thus, it is a multi-phonon process if $\omega_{max} < \frac{W}{\hbar}$, and is a single phonon process $\omega_{max} > \frac{W}{\hbar}$. In doped Ge, $\omega_{max} > \frac{W}{\hbar}$, indicating the hopping is a single phonon process (Miller and Abrahams 1960); Mott (1971) has suggested that because of the strong localization and lattice distortion in amorphous materials, high potential barriers would be

induced which are, in average, higher than the average energy of a single phonon; therefore, multiphonon process should be considered. However, no treatment for the case of $\frac{W}{h} > \omega_{max}$ has been reported at the present stage, the electronic frequency ν_{ph} can only be assumed to be of the same order of ω_{max}, which is about 10^{12} to 10^{13} sec^{-1}.

(iii) The wavefunction overlapping factor, in the form of $\exp(-2\alpha R)$

This factor is the measure of the overlap of the wave functions between two sites; it should be a decreasing function of spatial distance R, and also depends on the degree of localization of the sites. The coefficient α is a structural constant denoting the degree of localization of the sites.

It should be noted that at very low temperatures (say lower than 150°K) the electrons capable of hopping are those of order kT below E_F, and within this energy range all energy states can be assumed completely occupied. Therefore the electron concentration in this region is approximately equal to $N(E_F)kT$.

The probability per unit time for an electron to hop to a particular higher energy state with spatial distance R and energy difference W can be obtained by the product of these three factors (Mott and Davis 1971),

$$p = \nu_{ph} \exp(-2\alpha R - W/kT) \qquad (2.43)$$

Since the localized states are randomly distributed in space, the hopping motion must be a random motion and therefore can be statistically characterized by a diffusion coefficient D associatedwith the motion of Brownian particles. The diffusion coefficient has been given in

equation (2.15) for the diffusion of single Brownian particle hopping to random directions. The diffusion coefficient for an electron hopping to some particular state can be obtained by removing the spatial factor $\frac{1}{6}$, and we have

$$D = pR^2, \tag{2.44}$$

Using Einstein's relationship, the corresponding mobility is

$$\mu = \frac{eR^2}{kT} p, \tag{2.45}$$

the conductivity contributed by all the trapped electrons $N(E_F)\ kT$ is given by

$$\sigma = ne\ \mu \doteq e^2R^2p\ N(E_F). \tag{2.46}$$

By substituting equation (2.43) into equation (2.46), we have

$$\sigma \doteq \nu_{ph}\ e^2R^2\ N(E_F)\ \exp(-2\alpha R - W/kT). \tag{2.47}$$

We consider now the quantity W, the mean activation energy for hopping. First of all W is inversely proportional to the density of states (the larger the density of states, the smaller is the energy spacing between the states). Secondly, W depends on the radial distance between sites which are involved in the hopping. To relate R with W, we use the schematical diagram shown in Fig. 2.18. At very low temperatures, the phonon energy is small, so that the probability for the electrons to be activated by the phonon to a site with much higher energy is very small. Under this condition, as proposed by Mott, the energy difference between two hopping sites could be as small as the minimum energy

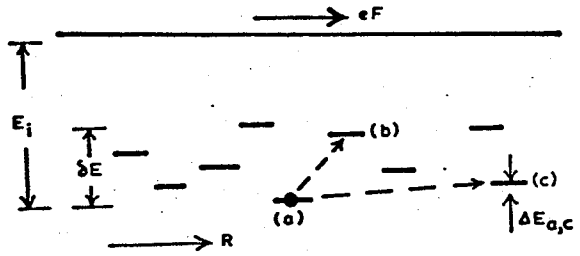

Fig. 2.18. Energy diagram of a localized band of empty traps. Trap (a) is the filled trap with negative charge. (After Hill, 1971).

separation, and the hopping distance R should be the maximum distance over which the electron can hop. Therefore, W can be assumed as the average energy difference between two states, which is,

$$W = 3/4\pi R^3 N(E_F) \tag{2.48}$$

and the radial distance required for the activation energy W in the hopping process is

$$R = \{3/4\pi W N(E_F)\}^{1/3} \tag{2.49}$$

Substituting equation (2.48) into equation (2.47), we obtain

$$\sigma \doteq \nu_{ph} e^2R^2 N(E_F) \exp\{-2\alpha R - 3/4\pi R^3 N(E_F)kT\} \tag{2.50}$$

The value of R can be estimated by the maximum conductivity condition

$$\frac{\partial \sigma}{\partial R} = 0 \tag{2.51}$$

Thus, we have

$$R_{max} = \{9/8\ \alpha\ \pi\ N(E_F)kT\}^{1/4} \tag{2.52}$$

Substituting equation (2.52) into equation (2.50), the conductivity becomes,

$$\sigma \doteq \nu_{ph} e^2R^2N \exp\{-(18\alpha^3/\pi N \cdot kT)^{1/4} - (\tfrac{3}{4})(\tfrac{8}{4})^{\frac{3}{4}}(\alpha^3/\pi N\ kT)^{1/4}\}$$

$$\doteq \nu_{ph} e^2R^2N \exp(-B/T^{1/4}) \tag{2.53}$$

with $B \doteq 2.1\ \{\alpha^3/N(E_F)kT\}^{1/4}$.

Equation (2.53) gives the relation $\ln \sigma \propto T^{-1/4}$ which is proposed by Mott (1969).

It is interesting to note that the $T^{-1/4}$ law holds even in the intermediate temperature range (say from 150°K to 250°K) provided that the

electron-electron interaction can be ignored (Hill 1971). According to Hill's arguments, there are only three major factors differ from Mott's model for the hopping conduction at higher temperatures:

(i) The hopping process may change from multiphonon process ($\omega_{max} < \frac{W}{\hbar}$) to single phonon process ($\omega_{max} > \frac{W}{\hbar}$) because ω_{max} increases with temperature.

(ii) Because the phonon energy increases with temperature, the "selection rule" of the low-temperature hopping conduction given by Mott should be changed accordingly. That is, the maximum hopping conductivity is determined by the activation energy W rather than by the hopping distance R, therefore, the maximum hopping conductivity is,

$$\frac{d\sigma}{dW} = 0 \tag{2.54}$$

and the hopping distance R is determined by the maximum activation energy W_{max} obtained from equation (2.54).

(iii) The trapped electron concentration cannot be assumed as $N(E_F)kT$, since the trapped electrons with energies much lower than E_F will participate in the hopping at higher temperatures. The electron concentration in this case is energy dependent, and can be expressed as $n_t(E)$.

By using the same procedures previously used for low temperature hopping conduction, and making the changes stated in (ii) and (iii) accordingly, we have (Hill, 1971)

$$\sigma \alpha \exp\{-2.31(2\alpha^3/\pi n_t kT)^{\frac{1}{4}}\} \tag{2.55}$$

which is of the same form as that for the low-temperature hopping conductivity in Mott's model.

2.10. Possible transport mechanisms for amorphous semiconducting covalent alloys

The basic transport mechanisms in amorphous semiconducting alloys have been recognized in the previous sections as the hopping of carriers among the localized states within the energy range of order kT near E_F at very low temperatures, and the wave-like propagation of carriers inside the conduction and valence bands at high temperatures. The experimental results on dc conductivity can be interpreted very well by using these two proposed mechanisms. However, in the transition temperature range (say from 150°K to 250°K), the experimental results cannot be interpreted so well by these two transport mechanisms as in the extreme temperature regions. It is therefore necessary to re-examine all possible mechanisms according to their contributions to the conductivity, in order to understand the characteristics of the conduction in the transition temperature region in more detail.

Böer (1970) summarized five possible transport mechanisms as follows:

(1) Propagation with occasional scattering.

(2) Diffusion-like propagation from neighbor to neighbor.

(3) Hopping amongst localized states, matching in energy within kT.

(4) Hopping amongst localized states including thermally excited states.

(5) Hopping amongst localized states of large energy differences activated by potential fluctuations.

These 5 transport mechanisms are schematically shown in Fig. 2.19. Mechanisms (1) and (3) have been discussed and recognized as the dominated transport mechanisms in high and extremely low temperature regions respectively. Mechanisms(2) is due to the carrier motion in the mobility shoulder region, and has

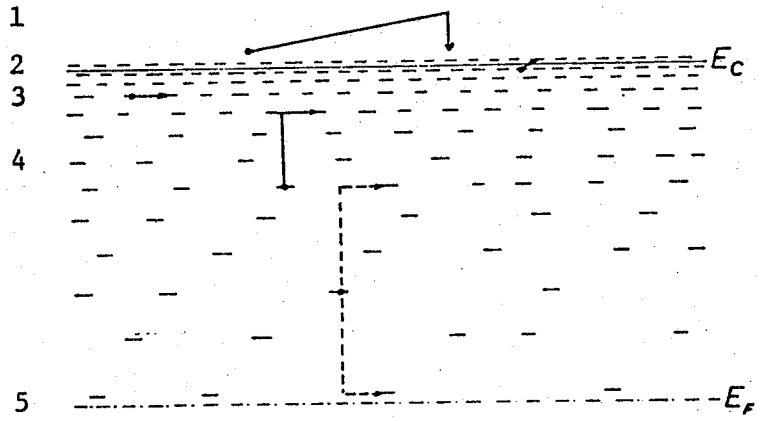

Fig. 2.19. Energy level distribution and possible transport mechanisms. (After Boer, 1970).

been termed by Cohen as Brownian motion (Part 1, equation (2.16)). Mechanism (5) is due to the tunneling of electrons from trap level to trap level activated by the potential fluctuations. The theory behind (5) is that tunneling from trap to trap is most probable for matching energies and decreases rapidly with increasing mis-match. Thermal broadening causes an increase of the probability of such matching, and the potential fluctuations provide another means for a shift of levels and give an opportunity for level matching. In highly disordered semiconductors these potential fluctuations may contribute markedly to level matching and consequently to tunneling.

If we assume that the dc conductivity is contributed by all these five mechanisms, we can write

$$\sigma = \sum_{i=1}^{5} \sigma_i = e \sum_{i=1}^{5} \int_{E_F}^{\infty} \mu_i(E)\, N(E)\, f(E)\, dE \qquad (2.56)$$

for n-type conduction; where σ_i, μ_i are the conductivity and mobility corresponding to the i^{th} mechanism. To evaluate the overall conductivity, we have to work out the magnitudes of the mobilities μ_i's corresponding to different mechanisms, then the corresponding σ_i can be estimated by the integral of equation (2.56). The overall conductivity is the sum of the contributions σ_i's obtained from all five mechanisms. Böer has roughly estimated the mobilities μ_i's and conductivities σ_i's, and the results as well as the μ_i, σ_i expressions are tabulated in Table 2.

In Table 2, a is the average interatomic separation N_t is the density of traps, ΔE is the energy difference between two trap states in the thermal excitation process, ν_σ is the fluctuation frequency factor approximately equal to $\sigma/\varepsilon\cdot\varepsilon_o$, R_f is the ratio of the band gap to the

Table 2. Summary of transport mechanisms in amorphous semiconductors

Transport mechanism (code)	Preferred energy region	Expression of Mobility μ	Expression of Conductivity σ	Estimated mobility ($cm^2/Vsec$)	Estimated conductivity $ohm^{-1}\ cm^{-1}$
1	$E \geq E_c + \varepsilon$ $E \sim 0.2$ eV $\lambda \geq a$	$\frac{e\lambda}{\sqrt{3kTm_n}}$	$eN_c(E_c+\varepsilon)x$ $\mu(E_c+\varepsilon)f(E_c+\varepsilon-E_F)$	~ 200	~ 5×10^{-6}
2	$E \sim E_c$ $\lambda \geq a$	$\frac{1}{6}(e/kT)a^2\nu$	$eN_{c\ 2}(E_c)\ x$ $f(E_c - E_F)$	~ 1	~ 10^{-9}
3	$E - E_F \sim kT$	$\frac{1}{6}(e/kT)R^2\nu_{ph}$ $x \exp(-z\alpha R)$	$eN_t(E_F)\ x$ $\exp(BT^{-1/4})$	~ 10^{-5}	~ 10^{-10}

Table continued...

Table 2. continued...

	$E_F < E < E_c$				
4		$\mu_3(\Delta E)\exp(\frac{-\Delta E}{kT})$	$e N_t \mu_3$ x $\exp[-\frac{(E_c - E_F)}{kT}]$	$\sim 10^{-3}$	$\sim 10^{-11}$
	$E_F < E < E_c$				
5		$\frac{1}{6}(e/kT)R_f^2\nu_\sigma$	$e N_t \frac{1}{6} \frac{e}{kT} R_f^2$ x $\nu_o \exp(-\frac{\Delta E}{kT})$	$\sim 10^{-6}$	$\sim 10^{-6}$

potential fluctuation energy, which equals to $(E_g/e\ N_t\ dV)$, and dV is the potential fluctuation from trap to trap.

PART 3. THE THERMOELECTRIC POWER OF CHALCOGENIDE GLASSES

The measurement of thermoelectric power or Seebeek coefficient is a powerful tool for investigating the electronic properties of solids, such as the band gap, the mobility ratio and the type of dominated carrier in semiconductors. Of most important application is that used for investigating charge transport phenomena in amorphous and high resistivity materials. We have discussed the transport mechanisms in chalcogenide glasses based on the temperature dependence of dc conductivity. However, the information deduced from dc conductivity is apparently not sufficient to predict the mechanisms beyond doubt. There are several transport properties such as optical absorption, high field effect, ac conductivity, thermoelectric power, photoconductivity etc., which are of importance to the formulation of transport theory. In this thesis, we shall discuss only the previous work on thermoelectric power measurement in addition to the dc conductivity.

2.11. The thermoelectric power (TEP or Seebeck coefficient)

Seebeck effect was discussed in 1822, which was the first thermoelectric phenomenon observed. TEP is normally measured using the circuit shown in Fig. 2.20a. The element I is made up of the sample to be tested while at B and C it is connected to the elements AB and CD of some high-conductivity metal II. The potential difference between A and D is measured by a suitable voltmeter with high input impedance. If all the elements in the system are at the same temperature, the potential

(a) Seebeck effect

$T_A \neq T_D$

$I = 0$

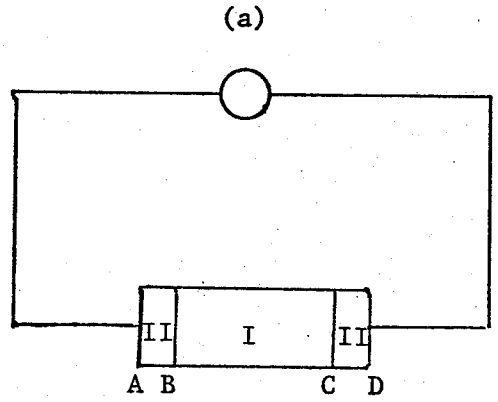

(b) Peltier effect

$T_A = T_D$

$I \neq 0$

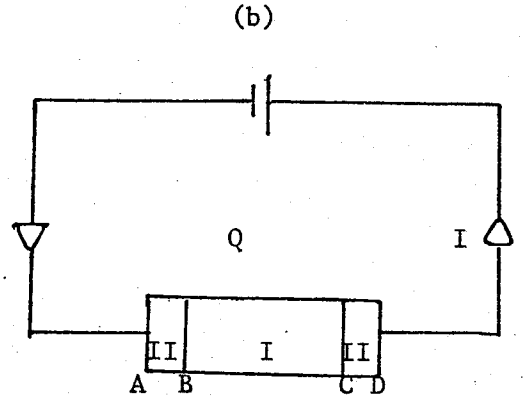

(c) Thomson effect

$T_A \neq T_D$

$I \neq 0$

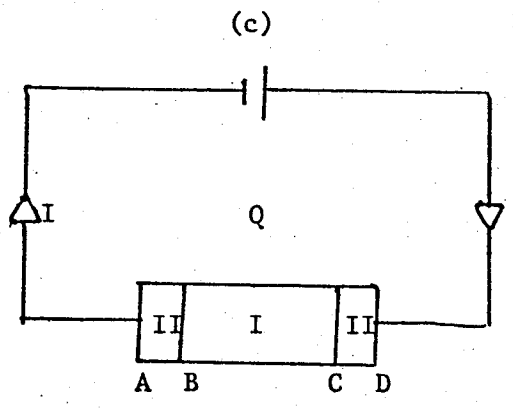

Fig. 2.20. Thermoelectric effects.

difference V_{AD} should be nearly zero. Seebeck (1822) found that if the temperatures at the junctions B and C are not the same, V_{AD} is of non-zero value. If the temperature at B junction is T, and at C is T + dT, then the potential between AD is dV. The following relation

$$S_{I,II} = \lim_{dT \to o} \frac{dV}{dT} \tag{2.57}$$

is defined as the differential Seebeck emf of the sample I and the metal II, or, the TEP of materials I and II. An obvious difficulty in defining this effect is to separate the contribution of the thermal voltage V_{AD} from these two kinds of materials I and II. Theoretically, no material can have a zero TEP at higher temperatures (say 300°K), because TEP is a measure of the diffusion of carriers due to the temperature gradient set up in the material (unless both carriers, electrons and holes, have the same density and effective mass). However, for some conductors with high thermal conductivity such as copper, gold, indium, etc., the TEP is very small compared with that for semiconductors, so that the contribution from these metals to the thermal voltage can be neglected, and the absolute TEP of the sample material can be determined. If the temperature gradient dT/dX is constant throughout the sample, we can write

$$S = \frac{\Delta V}{\Delta T} \tag{2.58}$$

where ΔV is the thermal voltage, ΔT is the temperature difference measured between the junction A and D, and S is the absolute TEP of the sample.

One of the important properties of TEP is that the type of dominated carriers in semiconductors can be determined by the polarity of the TEP.

The polarity of TEP is defined by

$$S \text{ is positive if } \frac{V_A - V_D}{T_A - T_D} < 0$$

$$S \text{ is negative if } \frac{V_A - V_D}{T_A - T_D} > 0 \qquad (2.59)$$

at junctions A and D.

Assuming that the majority carriers in the sample are of p-type, then if junction A is at higher temperature than D, both holes and electrons in the sample will tend to diffuse from junction B to C. As the hole concentration is much larger than the electron concentration, an excess hole concentration will set up near C. An electric field directed from C to B will set up and prevent further diffusion. Zero diffusion current indicates that an equilibrium has been reached. It is the electric field at equilibrium, which is completely responsible for the potential difference between A and D. It is obvious that for p-type materials the hot junction becomes negative with respect to the cold. By equation (2.59), the polarity of TEP is positive for p-type materials. Conversely, for n-type materials, the hot junction becomes positive, and thus gives a negative TEP.

2.12. The thermoelectric power in amorphous semiconductors

The most general form of TEP of amorphous semiconductors has been given by Culter and Mott (1969); in which the other two thermoelectric effects - the Peltier effect and Thomson effect - were involved. These two effects are briefly discussed in this section.

(A) The Peltier effect

Peltier effect discovered in 1834, is in fact the inverse of the

Seebeck effect. This effect assumes that initially the temperature through the sample is uniform, and a temperature gradient will set up by applying a dc field across the sample. Supposing that the temperature of the sample is initially uniform and a battery is connected to A and D as shown in Fig. 2.20b, then a current I will pass around the circuit. Peltier found that at one of the junction B or C, heat would be evolved and at the other, the same amount of heat would be absorbed. If the direction of applied voltage is reversed, the hot and cold junctions will interchange accordingly. A coefficient called the Peltier coefficient P is defined by

$$P = \frac{Q}{J} \tag{2.60}$$

where Q is the heat evolved per second and J is the current flowing through the sample.

It should be noted that the evolved heat Q in Peltier effect is independent of the Joule heat which does not depend upon the direction of the current. The Peltier coefficient is actually the measure of the total free energy carried by the carriers during the conduction, and therefore depends on the direction of the conduction of the majority carriers.

(B) The Thomson effect

Thomson effect was discovered as a result of thermodynamic studies of the relation between the Seebeck effect and Peltier effect. Thomson has shown that another effect must exist other than the first two to avoid violating the first and second law of thermodynamics. Thomson effect states that if a current J is flowing in a thermal conductor with a temperature difference ΔT between its two ends, then an amount

of heat will be evolved or absorbed in addition to the Joule heat. A coefficient called Thomson coefficient β^* is defined by

$$\beta^* = \frac{1}{J} \frac{\Delta J}{\Delta T} \tag{2.61}$$

where ΔQ is the amount of heat evolved or absorbed. β^* is taken as positive if the heat is evolved when a conventional positive current passes from the high to the lower temperature junction, and is negative if heat is absorbed.

Thomson's work lead to the following relations between the three thermoelectric effects (Putley 1960),

$$\beta^* = T \frac{dS}{dT} \tag{2.62}$$

$$P = TS \tag{2.63}$$

From equations (2.61) and (2.62), we have

$$\Delta Q = JT \, d \, S \tag{2.64}$$

and

$$Q = JTS \tag{2.65}$$

The thermoelectric effects in fact are dealing with the inter-relationship between the electrical and thermal transport of the carriers. Therefore Q is the total free energy transfer by the carriers.

(D) The general expression of dc conductivity

In Part 2, the dc conductivity at high temperature region (250°K and up) has been discussed; the conductivity in this region is assumed to be mostly contributed by the wave-like carriers. The most general expression of conductivity contributed by these carriers has been derived by Mott

and Davis (1971), which is given by

$$\sigma = - \int \sigma_E \frac{\partial f}{\partial E} dE \tag{2.66}$$

where σ_E is the conductivity contributed by the carriers with energy E, and f is the Fermi-Dirac distribution function which is given by

$$f = \exp\{-(E - E_F)/kT\} \tag{2.67}$$

because of the in-band conduction with the electron energies much higher than E_F, or, $(E - E_F) >> kT$.

The total amount of heat transfer in the material can be evaluated by means of equation (2.66), because the total heat transfer Q depends only on two basic quantities: the free carrier density and the energies carried by these carriers. If an external field F is applied, the total heat transfer is proportional to the field. The current dJ due to electrons with energies between E and $E + dE$ is given by

$$dJ = - \sigma_E \frac{\partial f}{\partial E} F \, dE \tag{2.68}$$

The free energy carried by dJ is

$$dQ = -(E - E_F) \, dJ/e$$

$$= \frac{F}{E} \sigma_E (E - E_F) \frac{\partial f}{\partial E} dE \tag{2.69}$$

and the heat transfer is:

$$Q = \frac{F}{e} \int_{E_c}^{\infty} \sigma_E (E - E_F) \frac{\partial f}{\partial E} dE \tag{2.70}$$

Using equation (2.65), we have

$$S = \frac{F}{Je} \int_{E_c}^{\infty} \sigma_E \, (E - E_F) \, \frac{\partial f}{\partial E} \, dE \tag{2.71}$$

Since $J = \sigma E$, we have

$$S\sigma = \frac{k}{E} \int_{E_c}^{\infty} \sigma_E \, \frac{(E - E_F)}{kT} \, \frac{\partial f}{\partial E} \, dE \tag{2.72a}$$

Equation (2.72a) is the general expression for TEP for n-type amorphous semiconductors (Culter and Mott, 1969).

Similarly, the general expression for TEP for p-type amorphous semiconductors can be written as

$$S\sigma = \frac{k}{e} \int_{-\infty}^{E_v} \sigma_E \, \frac{(E_F - E)}{kT} \, \frac{\partial f}{\partial E} \, dE \tag{2.72b}$$

In the high temperature region (250°K and up), in-band conduction is the dominant conduction mechanism, therefore we may assume

$$\begin{aligned} \sigma_E &= 0 \qquad \text{for} \quad E < E_c, \\ & \qquad\qquad\qquad\qquad \text{(n-type)} \\ \sigma_E &= \sigma_o + \alpha E \quad \text{for} \quad E > E_c, \end{aligned} \tag{2.73}$$

where σ_o is the pre-exponential factor of the dc conductivity, and

$$\begin{aligned} \sigma &= \sigma_o \exp[-(E_c - E_F)/kT] \qquad \text{(n-type)} \\ \sigma &= \sigma_o \exp[-(E_F - E_v)/kT] \qquad \text{(p-type)} \end{aligned} \tag{2.74}$$

Substituting equations (2.67), (2.73) and (2.74) into equation (2.72a), we have

$$S = \frac{k}{e} \left\{ \frac{E_c - E_F}{kT} + \frac{1 + 2kT(d\ell n\, \sigma/dE) + \ldots}{1 + kT(d\ell n\, \sigma/dE) + \ldots} \right\} \tag{2.75}$$

or

$$S = \frac{k}{e} \{\frac{E_c - E_F}{kT} + 1 + \text{terms of order } T\} \tag{2.76}$$

or simply,

$$S = \frac{k}{e} (\frac{E_c - E_F}{kT} + A_e) \quad \text{(n-type)} \tag{2.77a}$$

$$S = \frac{k}{e} (\frac{E_F - E_v}{kT} + A_h) \quad \text{(p-type)} \tag{2.77b}$$

in which A_e and A_h differ slightly for different materials, and are temeprature-dependent. However, according to Hindley's analysis using the random phase model (Hindley, Random phase model of amorphous semiconductors I and II, 1970), A_e and A_h have values approximately equal to unity.

The polarity of S is determined by the sign of e in equations (2.77a,b); for p-type materials, S is positive. Equations (2.77a,b) also indicate that the activation energies $(E_c - E_F)$ or $(E_F - E_v)$ can be determined by the temperature dependence of TEP. Defining ΔE_e and ΔE_h as the separations of the Fermi level from conduction and valence bands respectively, the TEP for either type of carriers is

$$S_{h,e} = \pm (\frac{k}{|e|}) [\frac{\Delta E_{h,e}}{kT} + A_{h,e}] \tag{2.78}$$

and if the temperature dependence of $\Delta E_{h,e}$ is assumed to be linear with T, following the relation

$$\Delta E_{h,e} = \Delta E_{ho,eo} - \beta_{h,e} T \tag{2.79}$$

then equation (2.78) becomes

$$S_{h,e} = \pm (\frac{k}{|e|}) [\frac{\Delta E_{ho,eo}}{kT} - \frac{\beta_{h,e}}{k} + A_{h,e}] \tag{2.80}$$

where $\Delta E_{ho,eo}$ is the separation of E_F from E_c or from E_v at $T = 0°K$.

For two-carrier conduction, the TEP is the difference of the weighted contributions from holes and electrons (Hindley 1970),

$$S = \frac{k}{|e|} \frac{\sigma_h[\frac{\Delta E_{ho}}{kT} - \frac{\beta_h}{k} + A_h] - \sigma_e[\frac{\Delta E_{eo}}{kT} - \frac{\beta_h}{k} + A_e]}{\sigma_h + \sigma_e} \qquad (2.81)$$

where σ_h and σ_e are respectively the hole and electron conductivities. The activation energy of TEP for two-carrier conduction is much more difficult to interpret than for one-carrier conduction. From equation (2.81), it is obvious that the activation energy for two-carrier conduction is smaller than that for one-carrier conduction. Despite of the types of conduction, the activation energy of TEP is easily determined from the slope of $S(T)$ versus T^{-1}, and they are

$$\Delta E_s = \Delta E_{ho} = E_F - E_v, \qquad \text{(one-carrier p-type)} \qquad (2.82a)$$

$$\Delta E_s = \Delta E_{eo} = E_c - E_F, \qquad \text{(one-carrier n-type)} \qquad (2.82b)$$

and

$$\Delta E_s = \frac{\sigma_h \Delta E_{ho} - \sigma_e \Delta E_{eo}}{\sigma_h + \sigma_e} = \frac{\sigma_h(E_F - E_v) - \sigma_e(E_F - E_V)}{\sigma_h + \sigma_e} \qquad (2.83)$$

(two-carrier)

If ΔE_s is related to the electrical activation energy ΔE_o obtained from the dc conductivity measurement and the conduction is of two-carrier type, ΔE_s must be smaller tha ΔE_s; since ΔE_s is smaller than either $(E_c - E_F)$ or $(E_F - E_v)$. However, this is not the only reason for ΔE_s smaller than ΔE_o; in fact, another factor arising from the mobility of the carriers is far more important. For simplicity, the carrier

mobility is frequently assumed to be independent of temperature, but this is actually not true. The electrical activation energy is not only responsible for the amount of thermal energy to excite the electrons to the conduction band, but also responsible for the amount of thermal energy to increase the mobility of the "in-band" carriers. Both energies contribute to the conductivity, and are therefore absorbed in ΔE_o. If the temperature dependence of miblity can be approximated by

$$\mu(T) = \mu_o \exp(-\Delta E_\mu/kT) \tag{2.84}$$

then we have,

$$\Delta E_o = \Delta E_{ho,eo} - \Delta E_\mu \tag{2.85}$$

where ΔE_μ is the activation energy of the temperature-dependent mobility.

In part 2 section 2.8, we use the intrinsic conduction approximation to find the p/n ratio, μ_p/μ_n ratio, etc. In this section, we use the same approximation to simplify the TEP expression, particularly in the case of two-carrier conduction. The assumptions are:

(i) E_F is located at the center of the gap, $\Delta E_{ho} = \Delta E_{eo}$

(ii) the temperature factors β_h and β_e are equal

(iii) $A_e = A_h$.

Based on these assumptions, the TEP for one-carrier and two-carrier intrinsic cases are summarized in the first column of Table 3. The second column is the activation energy ΔE_s related to ΔE_o in either cases by assuming temperature-independent mobility; the third column is the activation energy ΔE_s related to ΔE_o with the temperature-dependent mobility.

Finally, it is interesting to note that in the two-carrier intrinsic case with a constant mobility, the conductivity ratio can be estimated by the activation energies ΔE_h and ΔE_o from the following equation

$$\Delta E_s = \left(\frac{1 - \sigma_e/\sigma_h}{1 + \sigma_e/\sigma_h}\right) \Delta E_o \tag{2.86}$$

Moreover, if the conduction is of ambipolar, $n = p$ but $\mu_h \neq \mu_e$,

$$\Delta E_s = \left(\frac{1 - \mu_e/\mu_h}{1 + \mu_e/\mu_h}\right) \Delta E_o \tag{2.87}$$

the mobility ratio can also be estimated by ΔE_s and ΔE_o.

Table 3. The intrinsic approximation of TEP and the relation of ΔE_s, ΔE_o and ΔE_μ. (after Rockstad, Flasck and Iwasa, 1972)

Conduction Type	TEP S	ΔE_s For μ = constant $\Delta E_o = \Delta E_{ho} = \Delta E_{eo}$	ΔE_s For $\mu = \mu(T) = \mu_o \exp(-E/kT)$ $\Delta E_o = \Delta E_{ho,eo} - \Delta E_\mu$
Two-carrier intrinsic	$\frac{\sigma_h - \sigma_e}{\sigma_o + \sigma_e} \frac{k}{e} \left(\frac{\Delta E_{ho}}{kT} - \frac{\beta_h}{k} + A_h\right)$	$\frac{\sigma_h - \sigma_e}{\sigma_h + \sigma_e} E_o$	$\frac{\sigma_h - \sigma_e}{\sigma_h + \sigma_e} (\Delta E_o - \Delta E_\mu)$
One-carrier holes	$\frac{k}{e} \left(\frac{\Delta E_{ho}}{kT} - \frac{\beta_h}{k} + A_n\right)$	ΔE_o	$\Delta E_o - \Delta E_\mu$

By intrinsic approximation, $\Delta E_{ho} = \Delta E_{eo}$; $\beta_h = \beta_e$; $A_h = A_e$. The one-carrier expressions for electrons are exactly the same as those for holes.

CHAPTER 3

EXPERIMENTAL PROCEDURES AND TECHNIQUES

3.1. Experimental procedures for temperature-dependent dc conductivity measurements

Temperature-dependent dc conductivity of Ovonic glasses Ge_{10} Si_{12} As_{20} Te_{48} has been measured in a wide temperature range from 455°K to 161°K. To obtain high degree accuracy, the measurements were performed in a cryostat under a vacuum of about 10^{-6} torr. In this section the sample preparation and the measurement techniques are described as follows:

(A) Sample preparation

The amorphous Ge_{10} Si_{12} As_{30} Te_{48} glass was supplied by Malvern Radar Research Laboratories in England. The samples were produced by cutting the ingot into wafers, and then followed by the procedures given below.

(i) Polishing

The wafer was stuck firmly with wax on a copper block and then polished with 5 μm Al_2O_3 powder mechanically down to about 100 μm in thickness with mirror-like surfaces.

(ii) Thickness measurement

The thickness of the wafer was measured by a micrometer (Marcer model 112/521) with the accuracy of about $\pm$ 2.5%.

(iii) Cleaning and etching

The wafer was then rinsed in tricholethylene to remove the wax, and cleaned with alcohol and distilled water. Then the wafer was put in a solution of K_2 Cr_2 O_7 ($20cm^3$), H_2 SO_4 (85 cm^3) and H_2O (500 cm^3) for

chemical etching. After etching, the samples were cleaned again with alcohol and distilled water.

(iv) Electrode deposition

Molybdenum electrodes of about 0.1 μm in thickness were deposited on both sides of the sample using an electron gun under a vacuum of 10^{-8} torr in a Varian Ion ultra high vacuum system. A thin stainless steel mask with a window of 0.3 cm in diameter was used to give the electrode of the same size. To avoid overheating the sample during electrode deposition, a stainless steel block connecting to the water cooling system was in direct contact to the substrate as a heat sink. With the sample prepared in the above manner, the sample possessed high reproducible electrical properties.

(v) Sample mounting

The samples were fabricated in a sandwich configuration and mounted in a gold-plated metal package as shown in Fig. 3.1.

A small piece of indium was put on top of the gold-plated substrate and the whole package was heated in an oven filled with argon gas. The sample was then put on the top of the indium melt to make a good contact with the substrate through the indium. For the top molybdenum electrode a thin copper wire of 0.1 mm diameter was welded to it with indium using a microwelder. A small drop of epoxy was deposited on top of the molybdenum-indium electrode to mechanically support the contact arrangement. The copper wire were welded to the top molybdenum electrode and to the gold-plated substrate (used as a counter electrode), and with other ends welded to the outlet leads for electrical connection as shown in Fig. 3.1a.

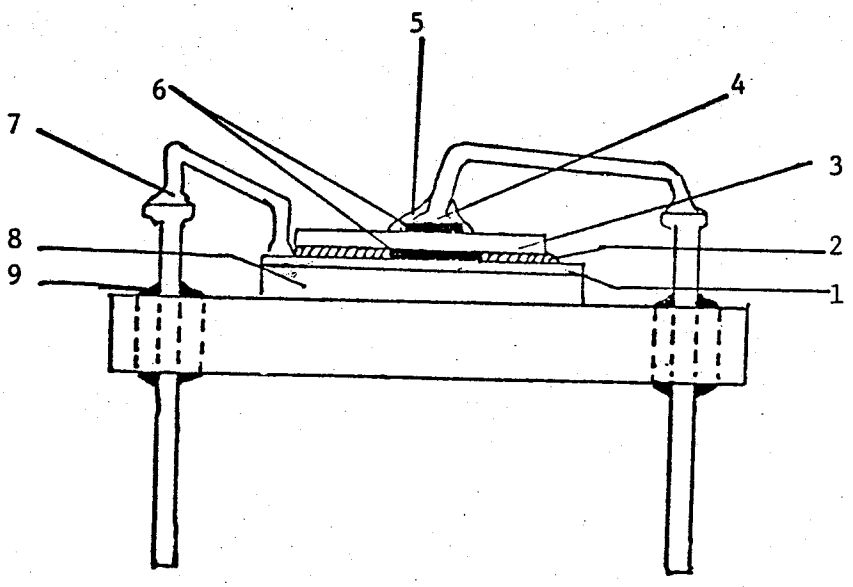

Fig. 3.1a. The sample and electrode arrangements.

1. gold-plated film of the substrate. 2. indium 3. sample. 4. indium welding. 5. epoxy. 6. molybdenum electrodes. 7. copper wire. 8. substrate. 9. lead insulation.

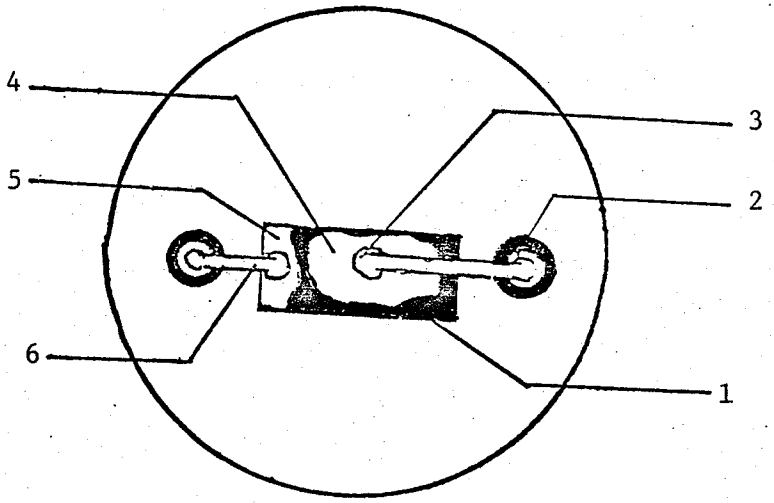

Fig. 3.1b. Top view of (a)

1. indium 2. copper wire and lead. 3. copper wire and electrod 4. sample. 5. gold-plated substrate. 6. copper wire.

(B) Temperature control arrangements

In order to have precise temperature control, a cryogenic dewar (Jauis Model 6-DT) was used. This equipment has double radiation shields to maintain a constant temperature in the sample compartment. The pressure in the sample compartment was maintained at 10^{-2} torr by a vacuum pump. The sample temperature was controlled by a solid-state temperature controller (cryogenic Research Model TC-103) with a platinum sensor. Detail arrangements were as follows:

(i) Sample and sensor mounting

A copper rod of 1.5 cm in diameter and 2 cm in length was used as the sample holder. Two holes of 1 cm and 0.2 cm in diameter were made at the bottom of the holder for sample and sensor mounting. The holes were filled with vacuum grease and then inserted with the sample and the sensor to assure perfect heat conduction between the holder, the sample and the sensor. The platinum sensor had four connections; two were connected to the temperature controller the other two were connected to the digital platinum thermometer (Hewlett Packard Model 2802A). All these connections were made with teflon-coated thin copper wires. To avoid possible damage to the sensor caused by heat, all connections were done by means of silver epoxy instead of soldering. The sample and sensor mounting are shown in Fig. 3.2a.

(ii) The temperature controller

A heater coil with 7.5 ohm resistance mounted just above the sample holder and was connected to the temperature controller. The temperature setability was within about 0.05°K which allowed the sample temperature to be reproduced with 0.5°K. The temperature control arrangements are shown in Fig. 3.2b.

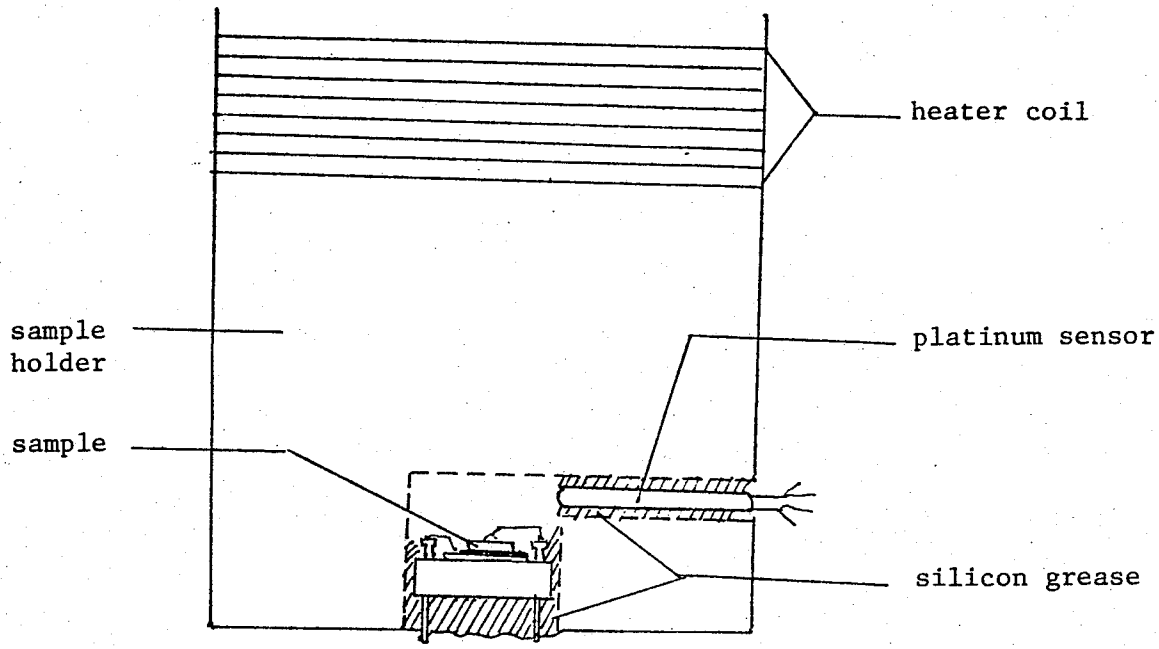

Fig. 3.2a. Sample and sensor mounting.

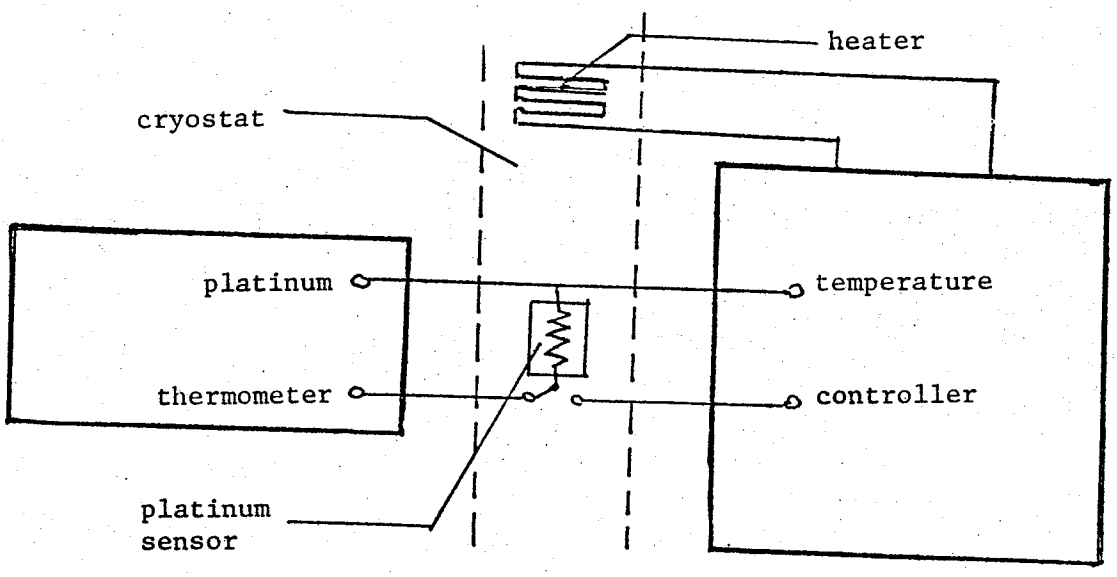

Fig. 3.2b. Temperature control and monitor arrangements.

(C) Electrical circuit

The electrical circuit used is shown in Fig. 3.3. Since the current at low temperatures was small (of the order of 10^{-12} ampere), shielded cables were used for all electrical connections in order to minimize possible disturbances. The sample current i_s was measured directly by the electrometer (Keithy 640 vibrating capacitor type). A pen recorder was also connected to the electrometer output to record the current so that the induced noise could be easily estimated. To minimize possible thermal emf which might introduced by dissimilar metal contacts, the copper wires were mechanically twisted and pressed together by means of a pair of tweezers, to avoid the effect of solders.

The dc conductivity is given by

$$\sigma = \frac{J}{\varepsilon} = \frac{i_s/A}{v_s/t} \tag{3.1}$$

where i_s is the current through the sample, v_s is the voltage drop across the sample, A is the area of the top electrode, and t is the thickness of the sample. When an electrometer was used as an ammeter, the input resistance was small, so the sample voltage v_s was equal to the voltage applied to the circuit.

(D) Experimental procedures

The most difficult part of dc conductivity measurement is that the conductivity changes markedly in a wide range from about 10^{-2} ohm^{-1} cm^{-1} at 455°K to about 10^{-13} ohm^{-1} cm^{-1} at 161°K. Marshall and Miller (1973) have reported that the dc conductivity of the Ge-Si-As-Te system is field-dependent, therefore the applied voltage in the temperature range

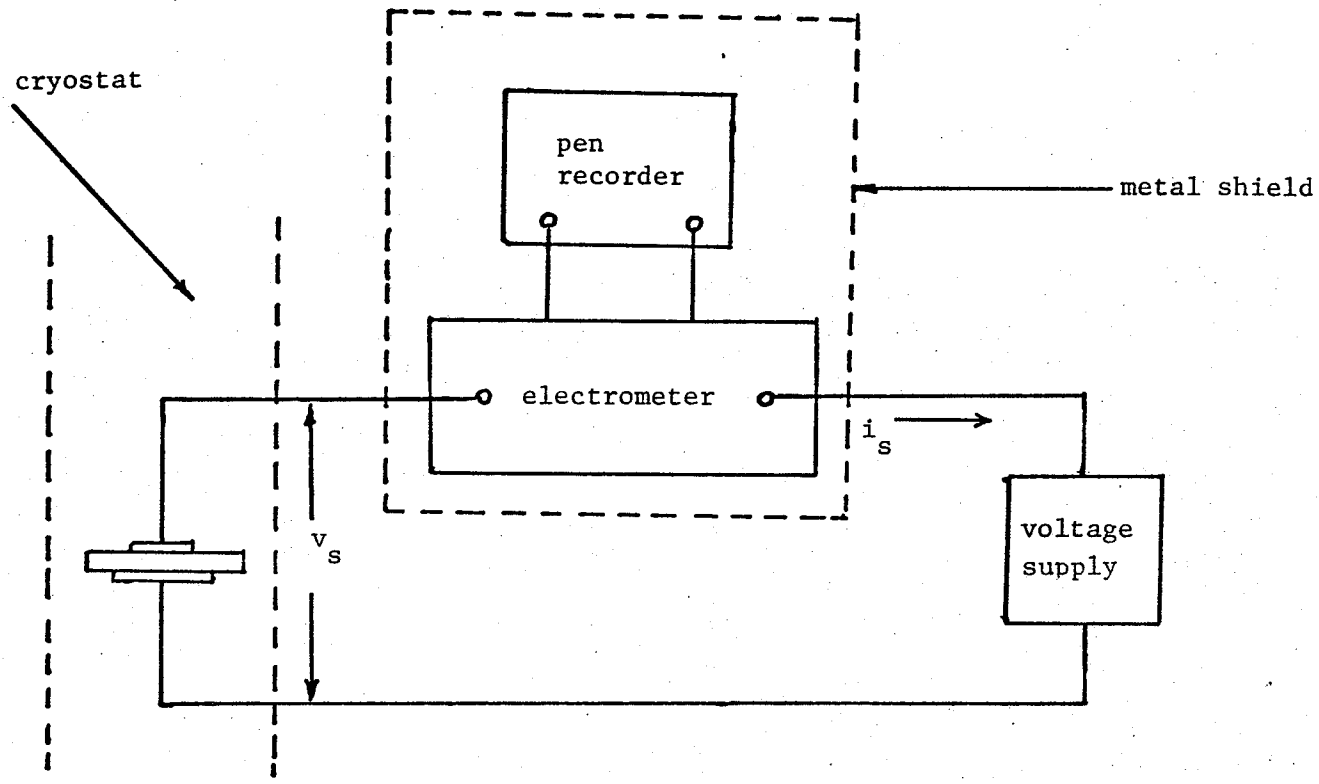

Fig. 3.3. The electrical circuit for dc conductivity measurements

under investigation must be kept constant. With a constant applied voltage, the current would change in almost 11 order within this temperature range. Furthermore, non-ohmic characteristics normally occur in the high temperature region (250°K and up) subjected to an applied field higher than 10^6 v/m. This would prevent an accurate measurement of the conductivity and make the analysis very complicate. Therefore the applied field was limited to less than 10^5 V/m. As the current was very small, the electrometer used for this measurement including the control header was shielded inside a metal box, and all shielded cable connections were kept short, rigid and straight.

The sample was then cooled in the cryostat chamber down to 161°K. By adjusting the temperature controller, the sample temperature was kept constant at this lowest point for one hour, the temperature was then increased step by step during the measurements. To assure temperature saturation, the sample temperature must be frequently checked and kept constant for not less than one hour before the current measurement was made. The measurement started from the lowest temperature (161°K) to the highest temperature (455°K) step by step, and then the measurement was repeated, but from the highest point to the lowest the same procedures were followed. The maximum deviation in the results between the heating process and the cooling process was about 7%. In general, the results were reproducible. Contact noise occurred in the low temperature region, the maximum noise being about 70% of the signal at 161°K. In fact, large contact noise is actually expected at these low temperatures as the sample current falls to the lowest range of the electrometer. However, despite of the magnitude of the noise, the

conductivity at these low temperatures measured are reproducible.

3.2. Experimental procedures and techniques for thermoelectric power measurement

Thermoelectric power was measured in the temperature range from 295°K to 415°K. The temperature gradient applied to the sample ranged from 1 deg/mm to 4 deg/mm. Since most of the TEP results are discrepant (for example, Kolomiets and Raspopova, 1972), a special measuring cell was designed to minimize the external influences in order to reduce the fluctuations of the measured Seebeck coefficient.

(A) Sample preparation

The sample Ge_{10} Si_{12} As_{30} Te_{48} was cut from the same ingot used for dc conductivity measurements. It was cut in the shape of a block with dimensions $3 \times 4 \times 10$ mm^3 using a diamond cutter. The top and bottom surfaces were polished manually with 5 μm Al_2 O_3 powder on a polishing cloth to produce mirror-like surfaces. The sample was then etched and cleaned following the same procedures described in section 3.1. The sample was then carefully examined under a microscope to check the surfaces, since irregular surfaces would prevent good mechanical contact with the indium spacers.

(B) The measuring cell

The cell was made of an aluminium tube and three pieces of glass tubings. The basic arrangements are shown in Fig. 3.4. The main purpose of the glass-tubing was to provide a good vacuum (the pressure in the sample compartment is less than 10^{-4} torr). The heat transfer to the sample under this vacuum was mainly contributed through the contacts of the heat sinks, therefore an uniform temperature gradient could be

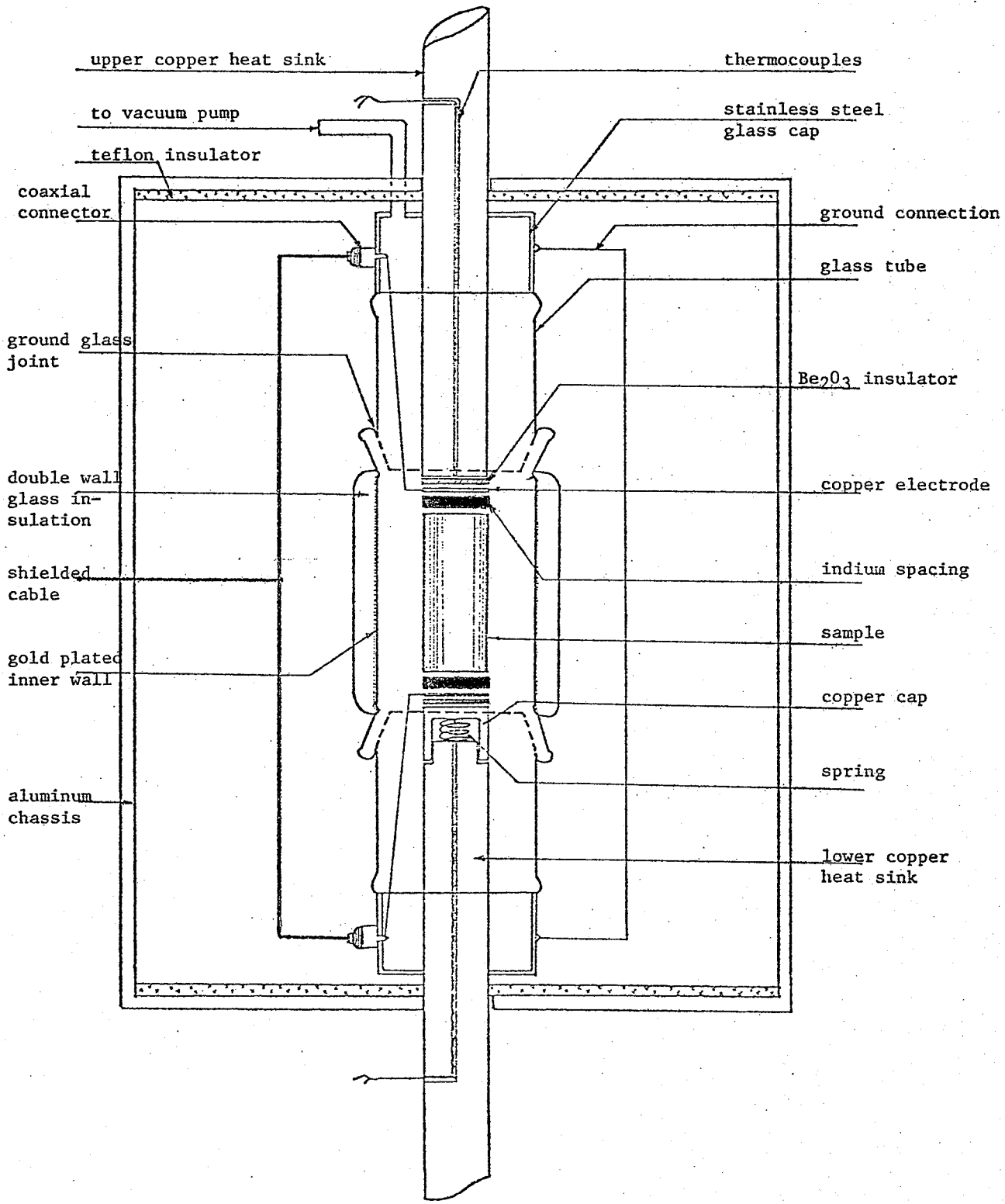

Fig. 3.4. Measuring cell for thermoelectric power measurement.

assumed within the sample. Furthermore, since it usually took more than ten days to complete one set of measurements, the sample compartment to be under a good vacuum to avoid possible oxidation at the sample surfaces and the indium spacers.

The glass tubing was composed of two identical stainless steel-glass jointed tubes and one double-walled gold-plated tube. These tubes could joined together through the greased glass joints to maintain good vacuum seals (less than 10^{-4} torr inside the tubing). The sample was located at the middle of the double-walled gold-plated tube, therefore heat and radiation influences from outside of the tubing on the sample were negligible.

Two copper rods each of 0.5 cm in diameter and of 30 cm length were used as heat sinks. The rods were hallowed and inserted with copper-constantant thermocouples which were attached to the inner tips of both rods. The rods were soldered to the ends of the stainless-steel tubes. A copper cap attached to a spring was put on the tip of one of the heat sinks to allow possible displacements due to heat expansion.

Since the sample is a high resistivity material, the insulation of the electrodes from the heat sink is important. Two thin pieces of $Be_2\ O_3$ of 0.5 mm in thickness and 0.5 cm in diamter were greased and inserted between the heat sinks and the electrodes for this purpose. The reason for the use of $Be_2\ O_3$ is that it is a very good thermal conductor as well as good insulator. The temperature difference between the heat sink and the $Be_2\ O_3$ surface on top of the heat sink was about 1.2°K at 400°K.

Two thin copper foils of 0.1 mm in thickness and 0.5 cm in diameter were used as electrical contacts. These foils were slightly

etched with diluted nitric acid before use. Between the sample and the contact, two indium disks of 1 mm in thickness and 0.5 cm in diameter were used as spacers to give good mechanical contact between the sample and the contacts. The indium spacers were machined to the shape of disks made of 99.99 pure indium wires, the surface of the disks were etched with H_2O_2 before use. Two teflon tubes of 0.5 cm in inner diameter were used to align the whole set of electrode and heat contact accessories in right direction.

The whole tubing with the heat sinks was put in an aluminum tube of 8 cm in diameter to avoid external electrical and radiation interferences. The heat sinks were extended outside of the aluminum tube and contacted to the teflon disks (of 5 cm in diameter) at the top and the bottom of the aluminum tube. Two aluminum disks (5 cm in diameter) with holes at the centre of a size slightly larger than the heat sink so that the heat transferred from the heat sink to the aluminum tube was small and would not affect the sample temperature.

The whole measuring cell was suspended vertically on a wooden frame. The lower heat sink was immersed in a thermostatically controlled silicon oil bath; and the upper heat sink was heated by heating coil with a well-regulated power supply.

The sample temperatures were measured with a millivolt potentialmeter (Cambridge L-361086). The thermal voltage was measured with an electrometer (Keithy Model 610).

For electrical connections, coaxial connectors were soldered on each stainless steel portion of the tubing; the electrodes were then connected to the connectors with 0.01 mm teflon coated copper wires. Double

shielded cables were used for the external connections, and were grounded to the aluminum tube. Furthermore, the top and bottom heat sinks were connected to each other with a copper wire so that the potential difference between them can be neglected.

A copper tube (1/4" diameter) was connected from the outside of the aluminum tube to the stainless steel portion, to provide an outlet for the vacuum pump connection. The external arrangements are shown in Fig. 3.5.

(C) Experimental procedures and techniques

The measurements of TEP, in principle, require merely the determination of a voltage and a temperature gradient of a suitably shaped sample. However, to achieve reliable results, certain precautions had to be made. The thermal voltage generally falls in the millivolt range or lower; the lower range of the electrometer usually is extremely sensitive to static pickup. In addition, the introduction of the means to heat the sample tends to result in instabilities and disturbances in the electrometer. The measuring cell used for the present investigation could eliminate part of the factors affecting the accuracy of the measurements. However, to reduce the scatter in the results, additional precautions are necessary. In the experiment, the whole measurements were completed in a double-screened and dark room, and all power supplies outside of the room. In addition, the following procedures were found to be absolutely necessary:

(i) The connection between the high ohmic electrometer input and the electrodes had to be kept short, rigid and straight.

(ii) The sample was pressed against the indium spacers when inserted and the contacts had to be tight enough to allow perfect heat conduction.

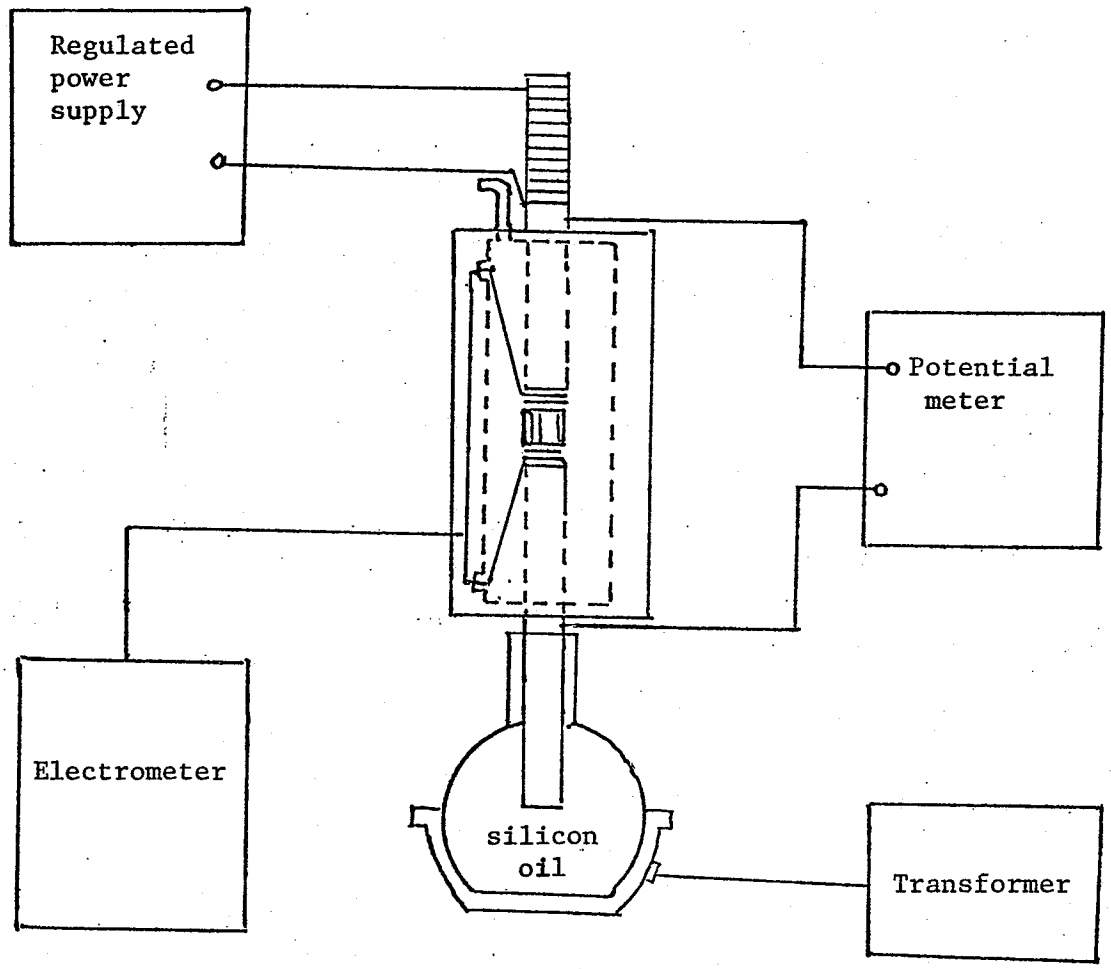

Fig. 3.5. The basic arrangements of TEP measurement.

(iii) The measurements were made after the sample had been kept in the dark compartment for 48 hours. In these measurements, the sample exhibited an emf as large as 50 mV when just inserted into the compartment; the emf reduced to 0.02 mV and became constant after it had been kept in the dark for two days. We took this emf (about 0.02 mV) as the zero point.

(iv) The temperature gradient applied was small (1 to 4 deg/mm)

(v) In order to obtain a constant temperature gradient across the sample - as far as possible - each temperature was kept constant for three hours. Each sample temperature and the thermal voltage were checked at least three times to assure that thermal equilibrium condition had been reached before the data was taken.

(vi) During the measurement several errors might arise, for example, the non-symmetrical configurations of the upper and lower electrode assembly, the diffusion of the contact material into the sample, annealing effect, and the poor contact due to the oxide layer between the sample and the indium spacers. These effects can only be roughly estimated by examining the reproducibility of the measurements, in fact, three basic procedures were found to be useful:

a. The sample had been cooled down and heated up within the temperature range interested for at least three cycles to see whether any irreversible change would have occurred.

b. The hot and cold electrodes were frequently reversed. This procedure was very effective to detect the non-symmetrical configuration of the upper and lower electrode assembly.

c. The Seebect coefficient can be determined by different temperature gradient $\left(= \frac{T_2 - T_1}{\ell} \right)$, where ℓ is the length

of the sample) at each ambient temperature ($= \frac{T_2 + T_1}{2}$). The value of the Seebeck coefficient should remain the same for different temperature gradients at about the same ambient temperature.

CHAPTER 4

EXPERIMENTAL RESULTS AND DISCUSSION

4.1. The dc conductivity

The temperature dependence of dc conductivity has been measured in the temperature range from 161°K to 455°K as shown in Fig. 4.1. The low temperature limit (161°K) was determined by the lowest conductivity of the sample, or in other words, the lowest current which could be measured with our available facilities. The high temperature limit (455°K) was determined by the melting point of the indium. The dc conductivity measured in this temperature range was very consistant in different heating and cooling cycles (c.f. section 3.1 (D)), the reproducibility for each value being within 7%.

The dc conductivity increases exponentially with increasing temperature in the whole temperature region following equation (2.20) as shown in Fig. 4.1. Using this plot; the electrical activation energy ΔE_o and the pre-exponential factor σ_o can be easily determined.

(A) The activation energy

Equation (2.20) gives,

$$\sigma = \sigma_o \exp(-\Delta E_o/kT) \tag{4.1}$$

or,
$$\ell n\, \sigma = \ell n\, \sigma_o - \frac{\Delta E_o}{kT} \tag{4.2}$$

Thus, we obtain

$$\Delta E_o = kT(\ell n\, \sigma/\sigma_o) \tag{4.3}$$

From Fig. 4.1, the slope of log σ versus $10^3/T$ has different

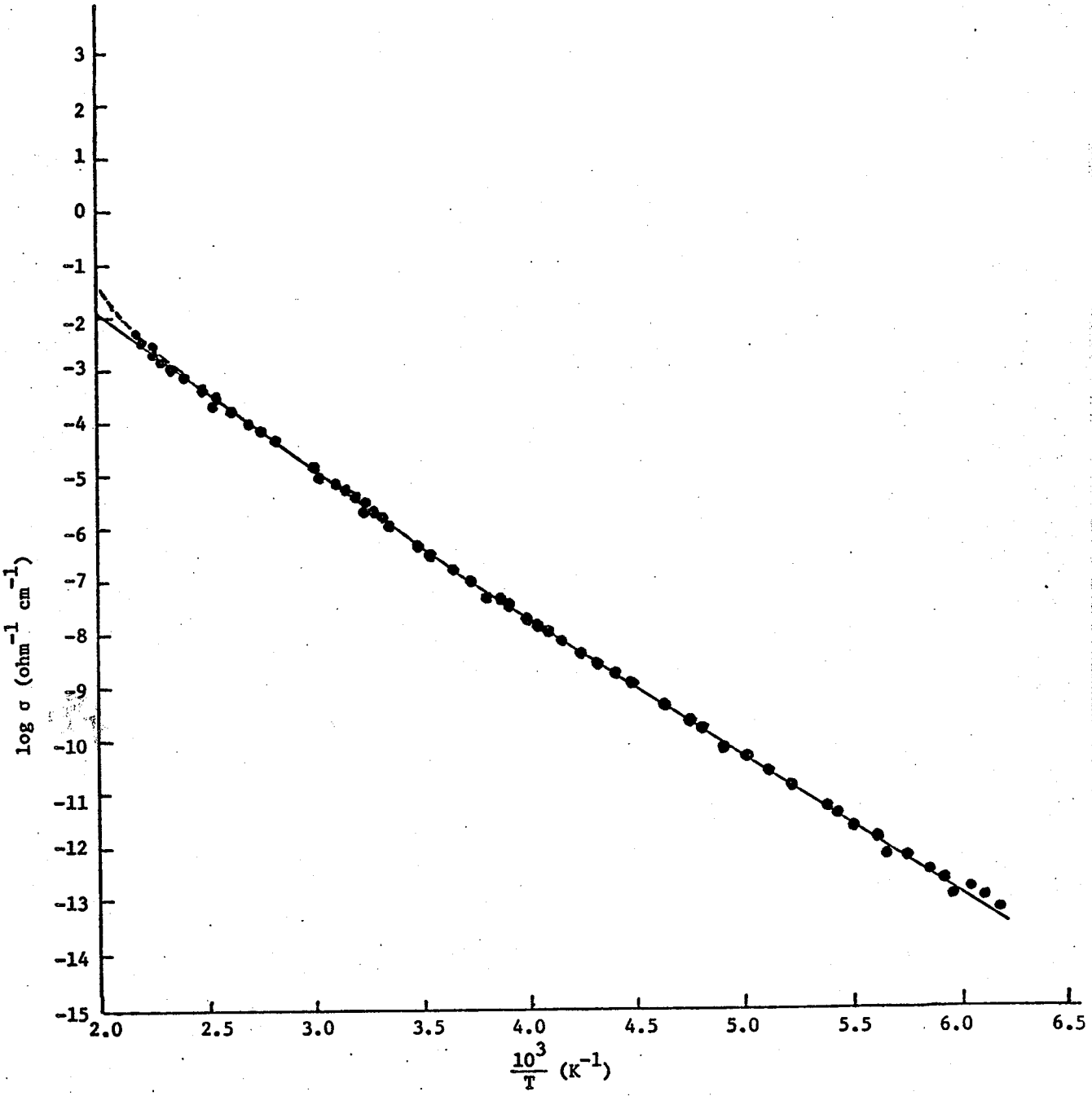

Fig. 4.1. Temperature dependence of dc conductivity of Ge_{10} Si_{12} As_{30} Te_{48}.

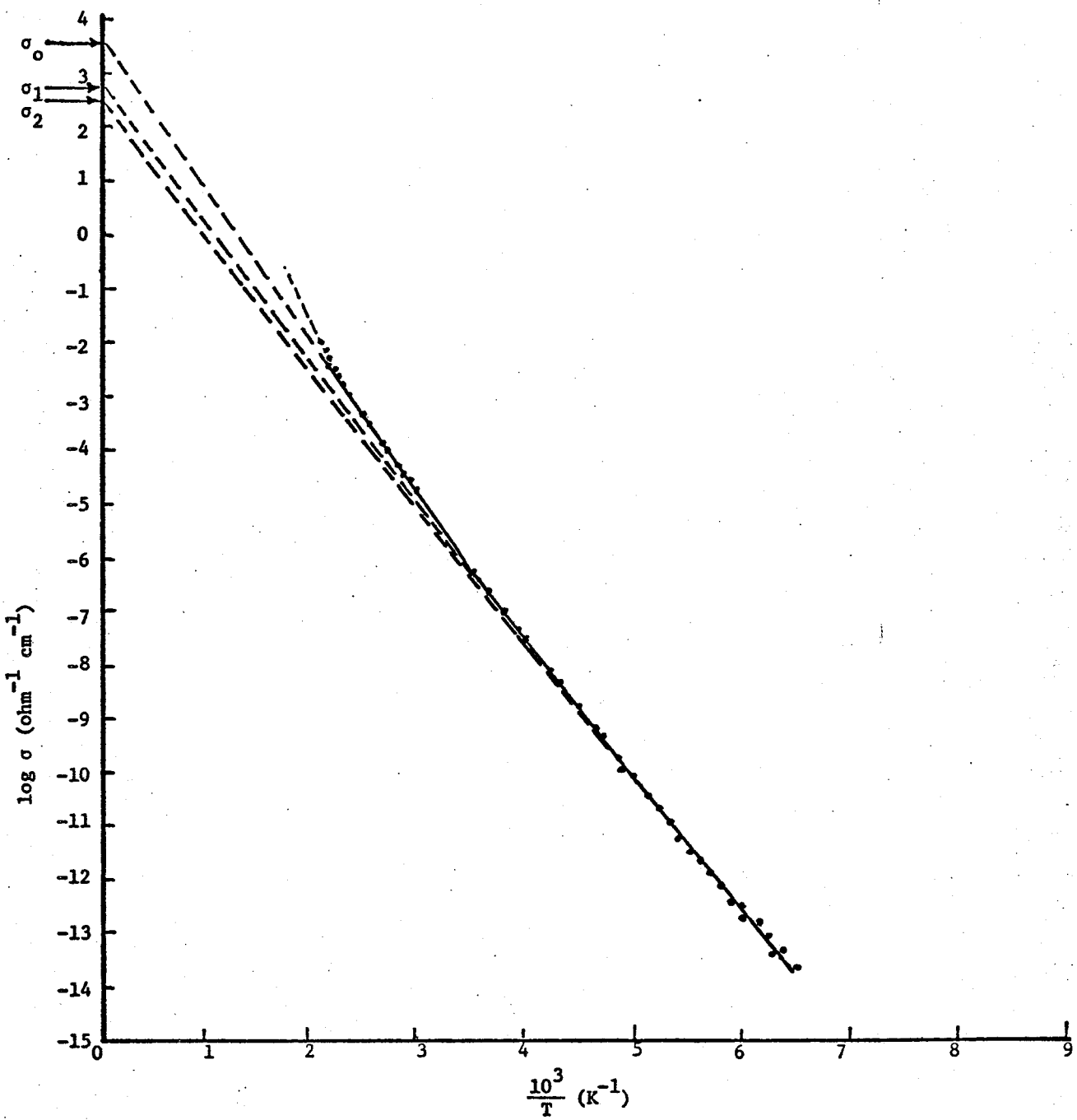

Fig. 4.2. The extrapolation of log σ at T = ∞.

values for different temperature regions, indicating that the activation energy has different values for these different temperature regions. For instance, in the temperature range from 444°K ($10^3/T = 2.25$, $\log \sigma = -2.69$) to 286°K ($10^3/T$, $\log \sigma = -6.20$), the slope yields the activation energy

$$\Delta E_o = 0.556 \text{ eV} \qquad (4.4)$$

The activation energies in these temperature ranges are summarized in Table 4.

Unfortunately, the activation energy at temperatures lower than 170°K could not be accurately determined because the conduction current at these temperatures had a large scattering. Also, in the temperature region higher than 444°K, the conductivity tended to increase rapidly, and the activation energy could be larger than 0.6 eV.

(B) The pre-exponential factor

The pre-exponential factor σ_o in equation (4.1) can also be obtained from equation (4.2) or simply by extrapolating $\log \sigma$ from the temperature range investigated to $T = \infty$. Since we have different activation energies associated with different temperature regions, the extrapolation of $\log \sigma$ should yield different σ_o in the corresponding temperature regions. The values of pre-exponential factors are also given in Table 4.

4.2. The thermoelectric power

In Fig. 4.3, the temperature dependence of TEP is plotted against 1/T in the temperature range from 400°K to 302°K. The TEP decreases linearly with increasing temperature in the whole temperature range. The scattering of the data is small compared with most of the TEP results reported by many investigators (for instance, Kolomiets and Raspopova 1971).

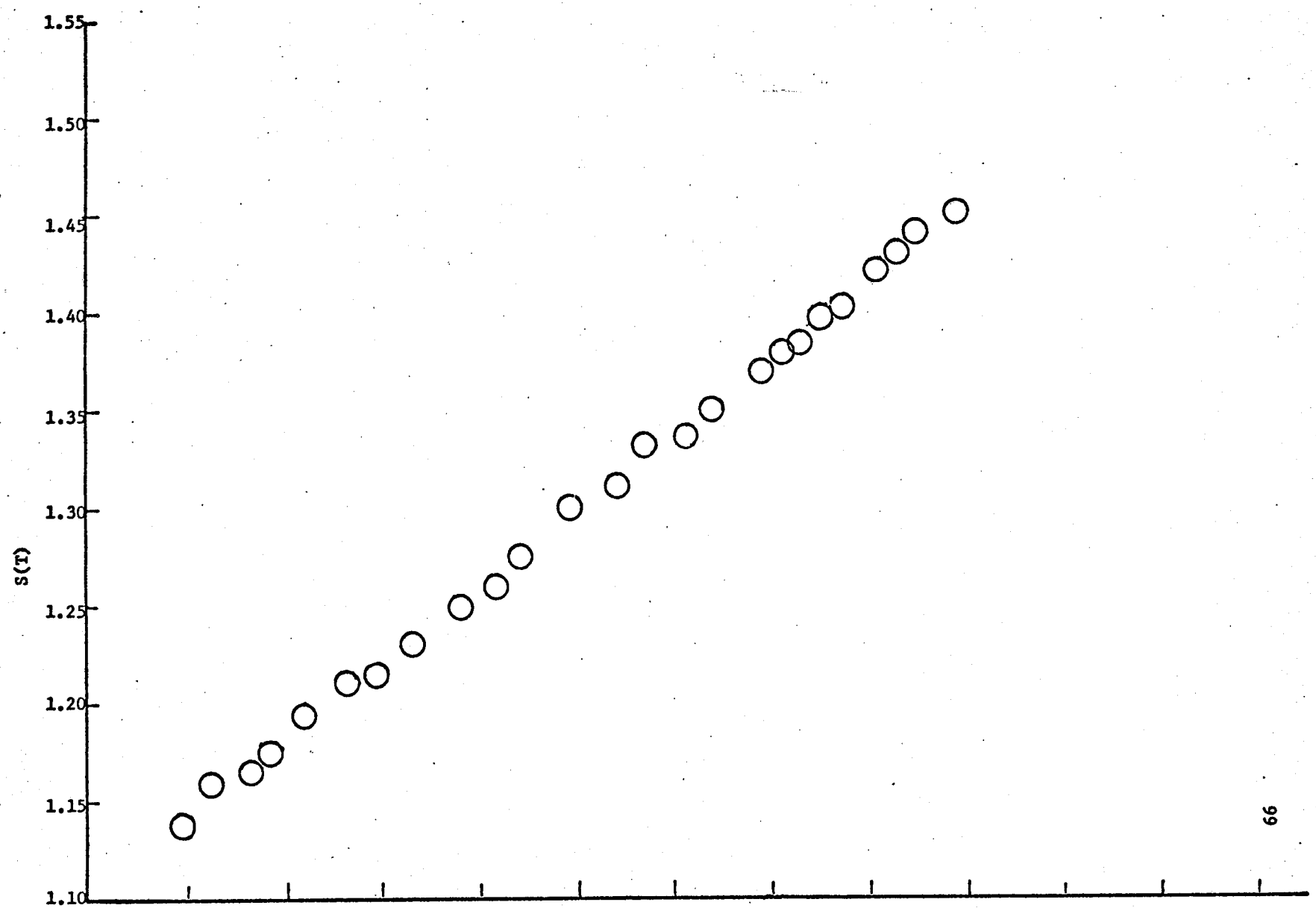

Fig. 4.3. Temperature dependence of TEP.

Table 4. The measured activation energies and pre-exponential factors

Temperature range	ΔE_o (eV)	σ_o ohm^{-1} cm^{-1}
444°K to 286°K	0.556	4.25×10^3
285°K to 210°K	0.515	7.08×10^2
209°K to 170°K	0.505	2.55×10^2

However, the scattering is still large enough to prevent a direct plot of TEP versus temperature based on a linear relationship. The slope of the S versus 1/T plot was determined by the method of least square (Neville and Kenneday, 1964). In this method, the relation of S(T) with T follows

$$S(T) = a + b\ (\frac{10^3}{T}) \tag{4.5}$$

where

$$a = \frac{\Sigma(\frac{10^3}{T})^2\ \Sigma S(T) - \Sigma(\frac{10^3}{T})\ \Sigma S(T)(\frac{10^3}{T})}{n\Sigma\ (\frac{10^3}{T})^2 - [\Sigma\ (\frac{10^3}{T})]^2} \tag{4.6}$$

$$b = \frac{n\Sigma\ S(T)(\frac{10^3}{T}) - \Sigma\ (\frac{10^3}{T})\ \Sigma\ S(T)}{n\Sigma\ (\frac{10^3}{T})^2 - [\Sigma\ (\frac{10^3}{T})]^2} \tag{4.7}$$

in which n is the total number of measurements; a is in mV K^{-1} and b is in mV so that S(T) is in mV K^{-1}. From equations (4.6) and (4.7) and with totally 25 TEP values measured, we have

$$a = 0.0954 \text{ mV } K^{-1} \tag{4.8a}$$

$$b = 414 \text{ mV} \tag{4.8b}$$

The TEP activation energy ΔE_s and the temperature factor β can be obtained from the values of a and b.

(A) TEP activation energy

Since the TEP decreases linearly with 1/T, which is in good agreement with equations (2.78) and (2.81); we can write

$$S(T) = \frac{k}{e}\ (\frac{\Delta E_s}{kT} - \frac{\beta}{k} + A) \tag{4.9}$$

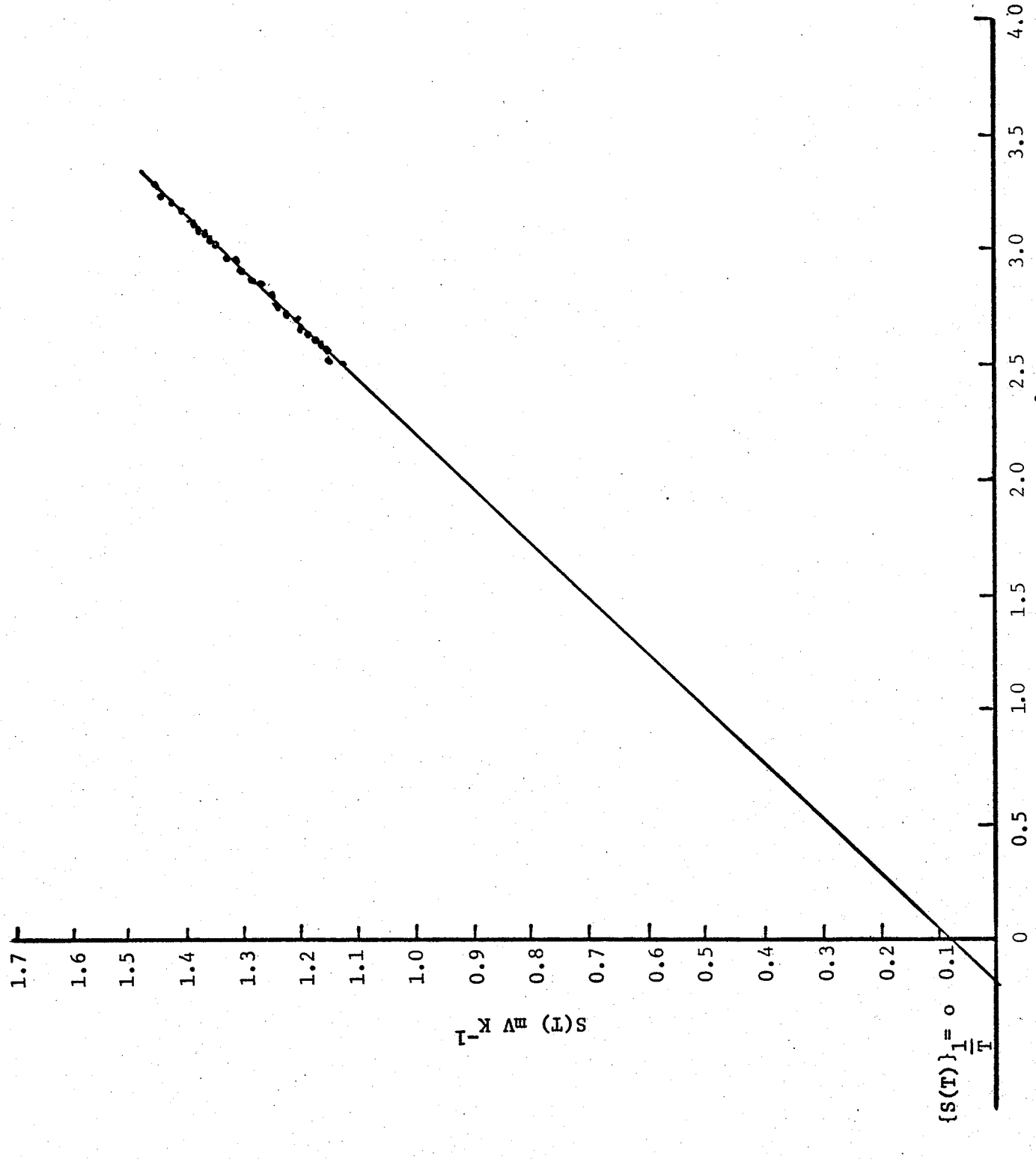

Fig. 4.4. The extrapolation of TEP at $T = \infty$.

the TEP activation energy can be obtained from the slope of the plot of S(T) versus 1/T with S(T) in mVK^{-1}. Equation (4.11) gives,

$$\frac{d\ S(T)}{d\ (\frac{1}{T})} = \frac{1}{e}\ \Delta E_s$$

or

$$\Delta E_s = e\ \frac{d\ S(T)}{d\ (\frac{1}{T})} = e \times \text{slope} \qquad (4.10)$$

The slope of the plot S(T) versus $10^3/T$ is the coefficient "b" given by the linear equation (4.5), and the calculated values in equation (4.8b). Thus we have

$$\Delta E_s = 0.414\ eV \qquad (4.11)$$

(B) The temperature factor β

β is the temperature dependence of ΔE_s and can be obtained by extrapolating S(T) from the temperature region investigated to $T = \infty$. Since the coefficient A is approximately equal to unity (Hindley 1970), from equations (4.5) and (4.9), we obtain

$$[S]_{\frac{1}{T}\to o} = (\frac{k}{e} - \frac{\beta}{e}) = a \qquad (4.12)$$

The extrapolation of S(T) to $10^3/T \to o$ gives the coefficient a from equation (4.5). Thus from the value of a given in equation (4.8a) and equation (4.12), we have

$$\beta = 9.2 \times 10^{-6}\ eV\ K^{-1} \qquad (4.13)$$

(C) The polarity of TEP

The polarity of TEP in the whole temperature range is consistent

with the lower and negative potential at the higher temperature end. This gives a positive TEP and indicates that the dominated carriers in Ge_{10} Si_{12} As_{30} Te_{48} are holes. It should be noted that the polarity of TEP was very sensitive to the temperature gradient, also the result was very consistent by reversing the hot and cold electrodes at various temperatures.

4.3. Discussion

The results based on the dc conductivity measurement summarized in Table 4 are in good agreement with the results of Male (1970) and the results of Marshall and Miller (1973). Marshall and Miller have reported that the activation energy for Ge_{10} Si_{12} As_{30} Te_{48} is 0.55 eV at 500°K and 0.50 eV at 160°K. The results based on the TEP measurements are also similar to those of Rockstad et al. (1972) for Ovonic glass Ge_7 Si_{18} As_{35} Te_{40} which has a TEP activation energy of 0.41 eV.

(A) The type of conduction carriers

The TEP measurements show that the conduction is of p-type. It is not easy to distinguish between the case of overwhelmingly one-carrier hole conduction and that of two-carrier conduction but definitely dominated by holes. The magnitude of the measured TEP in the temperature investigated is large (about 1.3 mV K^{-1}) which may be in favor of the one-carrier hole conduction.

The type of conduction can be further examined by comparing the conductivity results with the TEP results. Two assumptions are considered as follows:

(i) One-carrier p-type conduction

The difference between conductivity activation energy and the

TEP activation energy yields the activation energy for the mobility, therefore

$$\Delta E_\mu = \Delta E_o - \Delta E_s = (0.556 - 0.414)\ eV$$

$$= 0.142\ eV \qquad (4.14)$$

The activation energy for the mobility ΔE_μ at this high temperature region (400°K to 303°K) seems slightly larger than expected. Since the dominated transport mechanism in this temperature region is most likely due to in-band conduction. the mobility for in-band conduction would possibly follow equation (2.39)(c.f. section 2.8) rather than increases exponentially with T. If an exponential temperature dependence for mobility does occur, the corresponding energy should refer to the mobility shoulder and be about a few kT. However, Bube et. al. (1972) have suggested that the temperature dependence of mobility would follow an exponential form with an activation energy ranging from 0.05 to 0.2 eV based on their photoconductivity analysis. The value $\Delta E_\mu = 0.142$ eV obtained based on the one-carrier p-type assumption is very well within this range.

The type of conduction can also be examined by finding the pre-exponential factor σ_o. From equations (2.20) and Table 3, we have,

$$\sigma = \sigma_o \exp\left(-\frac{\Delta E_s + \Delta E_\mu}{kT}\right) \qquad (4.15)$$

$$S = \frac{k}{e}\left(\frac{\Delta E_s}{kT} - \frac{\beta_h}{k} + 1\right) \qquad (4.16)$$

For this case we can write,

$$\Delta E_s = \left(\frac{\sigma_h - \sigma_e}{\sigma_h + \sigma_e}\right) \Delta E_o \tag{4.19}$$

with $\Delta E_\mu = o$. Using the experimental results for ΔE_o and ΔE_s, the ratio of conductivities contributed by holes and electrons is

$$\frac{\sigma_h}{\sigma_e} = 6.843 \tag{4.20}$$

The contribution of holes is approximately seven times larger than that of electrons, which is significant to show a p-type conduction. Since $\Delta E_\mu = o$, equation (4.17) becomes

$$\sigma = \sigma_o \exp\left(-\frac{eS}{kT} + 1 - \frac{\beta_h}{k}\right) \tag{4.21}$$

Using the values of σ and S at 303°K, we have

$$\sigma_o = 29.38 \text{ ohm}^{-1} \text{ cm}^{-1} \tag{4.22}$$

which is too small compared with the measured σ_o obtained from the dc conductivity measurement. Therefore, we may conclude that if the conduction is a two-carrier intrinsic conduction, the activation energy for the mobility should not be assumed to be zero, or σ_o is too small to be reasonable.

b. Two-carrier, p-type conduction with an exponential temperature dependence for the mobility.

For this case, we can write,

$$\Delta E_s = \left(\frac{\sigma_h - \sigma_e}{\sigma_h + \sigma_e}\right)(\Delta E_o - \Delta E_\mu) \tag{4.23}$$

Substitution of equation (4.16) into equation (4.15) gives,

$$\sigma = \sigma_o \exp\{-\frac{(eS_T + \beta_h T - kT) + \Delta E_\mu}{kT}\} \qquad (4.17)$$

From equation (4.17), σ_o can be determined using σ and S from the experimental results and ΔE_μ based on the assumption of the type of conduction given by equation (4.14). Thus with $T = 303°K$, $S = 1.455$ mV K^{-1}, $\sigma = 4.17 \times 10^{-6}$ ohm^{-1} cm^{-1} and $\Delta E_\mu = 0.142$ eV, we have

$$\sigma_o = 6.73 \times 10^3 \text{ ohm}^{-1} \text{ cm}^{-1} \qquad (4.18)$$

The value of σ_o obtained from the extrapolation of σ at the same temperature region to $T = \infty$ is about 4.25×10^3 (Table 4), which is in good agreement with the calculated σ_o in equation (4.18) based on the one-carrier p-type assumption. The small difference between these two values may arise from the experimental deviation caused by using different samples in TEP and dc conductivity measurements. Therefore, the conduction is possibly be one-carrier p-type conduction.

(ii) Two-carrier conduction with p-type dominant.

It has been recognized (c.f. section 2.7), that the exponential temperature dependence of the conductivity at high temperatures s one of the evidence to favor the in-band conduction mechanism. Therefore the conduction is very likely an in-band conduction in this temperature region. There are two possible cases for the two-carrier in-band conduction as listed in Table 3.

a. Two-carrier, p-type intrinsic conduction with a non-exponential temperature dependence of mobility.

Since both the ratio of the conductivities and the mobility activation energy are not known, we can not obtain ΔE_μ directly. However, we can determine ΔE_μ by using equation (4.17), with $\sigma_o = 4.25 \times 10^3$ ohm^{-1} cm^{-1} found from the conductivity measurements. Thus,we have

$$\Delta E_\mu = 0.1299 \text{ eV} \tag{4.24}$$

Substituting equation (4.28) into (4.27), we have

$$\frac{\sigma_h}{\sigma_e} = 69.43 \tag{4.25}$$

the conductivity contributed by holes is much larger than by electrons. In fact, with this large ratio of conductivities, the conduction is completely dominated by holes rather than by two-carrier conduction.

Based on the above arguments, it is most likely that the conduction is of p-type one-carrier conduction, having an exponential temperature dependence of mobility with the activation energy ΔE_μ ranging from 0.130 eV to 0.142 eV.

(B) The mobility gap and the location of Fermi level

We have examined the possible type of conduction and determined that the conduction in our samples is of p-type one-carrier conduction. The intrinsic model proposed by Böer (c.f. section 2.8) based on an ambipolar conduction with the Fermi energy E_F located at the center of the mobility gap cannot interpret very well our experimental results. On the other hand, the model, put forward by Fritzsche (1970, 1971), which suggests that the Fermi level is not necessary be located at the gap center and also either holes

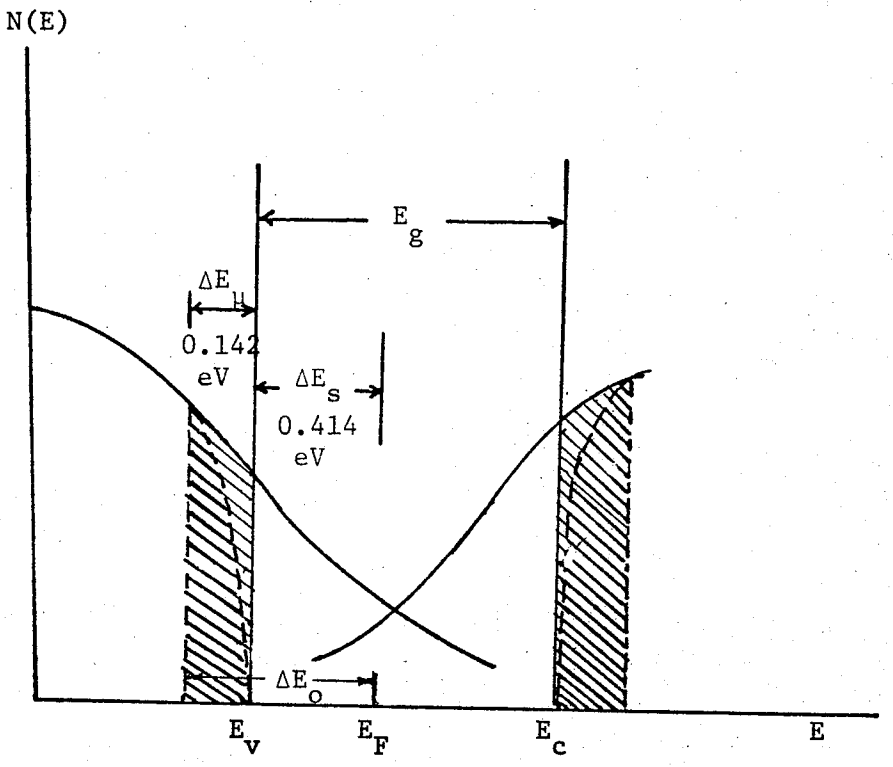

Fig. 4.5. The proposed band structure for Ge_{10} Si_{12} As_{30} Te_{48} at high temperatures. The cross-hatched region is the mobility shoulder.

or electrons should overwhelmingly dominate the conduction, is more applicable to our results. Therefore, we suggest that the Fermi energy level in Ge_{10} Si_{12} As_{30} Te_{48} under investigation may shift slightly towards E_v according to the overwhelming hole contribution. However, the amount of energy shifted can by no means be determined from our experiments, since there is no explicit relation between $(E_F - E_v)$ and the band gap. The activation energy ΔE_s which is equal to $(E_F - E_v)$ reveals only the information of the amount of energy required to excite a significant concentration of holes to the valence band edge to make the in-band hole conduction dominant in the temperature range from 400°K to 303°K. The electrical activation energy ΔE_o (0.556 eV) can be considered as the amount of energy required to create holes to valence band edge, and, activate the holes through the mobility shoulder to the effective in-band level (c.f. section 2.5). The proposed band structure is schematically shown in Fig. 4.5.

(C) The possible transport mechanisms

The dc conductivity decreases from 0.556 eV in the high temperature region (444°K to 286°K) to 0.505 eV in the low temperature region (210°K to 170°K) indicates that the in-band conduction mechanism at high temperatures could have been shifted partially to some other mechanisms when the temperature is falling towards the low temperature region. Since the temperature dependence of dc conductivity follows an exponential relationship in the whole temperature range (from 444°K to 170°K), it seems most reasonable to assume that the measured conductivity is contributed by all the transport mechanisms which require an exponential temperature dependence of conductivity. There are two possible transport mechanisms other

than in-band conduction mechanism which require an exponential temperature dependence of conductivity.

(i) The conduction due to carriers excited into the localized states near the valence band edge.

In certain temperature region, the phonon energy is not large enough to activate a band to band excitation, then the excitation would majorly take place in the gap region rather than in the valence band. If the phonon energy is not so low, i.e., only several kT lower than band to band activation energy, then a large concentration of holes could be activated to some energy level E_v' which is of the order of kT above E_v. These holes would then hop over the energy barrier $(E_v' - E_v)$ and significantly contributed to the conductivity. The conduction via the process should follow the relation

$$\sigma = \sigma_1 \exp\{-(E_F - E_v' + \Delta W_1)/kT\} \qquad (4.26)$$

where ΔW_1 is the activation energy for hopping. The activation energy $(E_F - E_v' + \Delta W_1)$ must be smaller than $(E_F - E_v + \Delta E_\mu)$, otherwise the band to band conduction would take over conduction. Mott and Davis (1971) have estimated that the pre-exponential factor σ_1 is about 10^2 to 10^4 less than σ_o for the in-band conduction. The drop of σ_1 is due partly to the lowering of the effective density of states at the level E_v' by a factor $(E_v' - E_v)/kT$, but due mainly to the mobility drop in the mobility shoulder.

(ii) The hopping conduction between nearest neighbors near E_F.

At extremely low temperatures, the hopping conduction is characterized by the $T^{-\frac{1}{4}}$ law, and the electrons hop to a large distance to the lower energy sites. In the intermediate temperature region (150°K to 250°K) the hopping process is changed from a multiphonon process ($\omega_{max} < \frac{W}{\hbar}$) to a single-phonon process ($\omega_{max} > \frac{W}{\hbar}$) (c.f. section 2.9), which is analogous to the impurity conduction in heavily-doped crystalline semiconductors. The expression for the hopping conductivity thus takes the same form for the impurity conduction;

$$\sigma = \sigma_o \exp(-\Delta W_2/kT) \tag{4.27}$$

where ΔW_2 is the mean activation energy for hopping. Since in the single-phonon process, $\omega_{max} > \frac{W}{\hbar}$, the electrons would hop to its nearest neighbors despite of the potential barriers; and also the localized states are randomly distributed in space, therefore ΔW_2 is about a few kT smaller than $(E_F - E_v)$, and the pre-exponential factor σ_2 is about 1 order less than σ_1. The dc conductivity may then be written as

$$\sigma = \sigma_o \exp(-\frac{\Delta E_o}{kT}) + \sigma_1 \exp\{-\frac{(E_F - E_v' + \Delta W_1)}{kT}\} + \exp(-\frac{\Delta W_2}{kT}) \tag{4.28}$$

Our experimental results give only the activation energies and pre-exponential factors, and are apparantly not sufficient to estimate

quantitatively the contributions from these independent transport mechanisms to the conductivity. However, a rough estimation can be made to see the tendency of the shifting of these transport mechanisms based on some assumed values of σ_1, σ_2, E_v', ΔW_1 and ΔW_2. Assuming $(E_v' - E_v) = 2kT$, $\Delta W_2 = (E_F - E_v) - 3kT$, $\sigma_1 = \sigma_o \times 10^{-4}$, $\sigma_2 = \sigma_o \times 10^{-5}$, and $\Delta W_2 \doteqdot 0.09$ eV (suggested by Ormondryd et. al. 1974), we estimate the corresponding conductivites as follows

(a) $\sigma(o) = \sigma_o \exp(-\Delta E_o/kT)$

with $\Delta E_o = 0.556$ eV $\quad \sigma_o = 4.25 \times 10^3$ ohm^{-1} cm^{-1} we have

at 444°K $\quad \sigma(o) = 2.1 \times 10^{-3}$ ohm^{-1} cm^{-1} (4.33)

at 285°K $\quad \sigma(o) = 1.53 \times 10^{-1}$ ohm^{-1} cm^{-1} (4.34)

at 160°K $\quad \sigma(o) = 1.59 \times 10^{-13}$ ohm^{-1} cm^{-1} (4.35)

(b) $\sigma(1) = \sigma_1 \exp\{-(E_F - E_v' + \Delta W_1)/kT\}$

with $(E_F - E_v) = \Delta E_s = 0.414$ eV, $\sigma_1 = \sigma_o \times 10^{-4} = 0.425$ ohm^{-1} cm^{-1} we have

$$(E_F - E_v') = 0.414 \text{ eV} - 2kT \tag{4.38}$$

and

$$\Delta E_1 = 0.414 + 0.09 - 2kT$$

$$= 0.423 - 2kT \tag{4.39}$$

In the whole temperature range from 444°K to 170°K, ΔE_1 is ranging from 0.394 to 0.346 eV. The average value of ΔE_1 is about 0.37 eV, which is small compared with ΔE_o (0.556 eV).

Thus, the contribution to conductivity is

at 444°K $\sigma(1) = 2.72 \times 10^{-5}$ ohm^{-1} cm^{-1}

at 285°K $\sigma(1) = 1.3 \times 10^{-7}$ ohm^{-1} cm^{-1}

at 170°K $\sigma(1) = 4.98 \times 10^{-12}$ ohm^{-1} cm^{-1}

(c) $\sigma(2) = \sigma_2 \exp(-\Delta W_2 / kT)$

With $\Delta W_2 = 0.414 - 3kT$, ΔW_2 has an average value about 0.335 eV, and $\sigma_2 = \sigma_o = 0.0425$ ohm^{-1} cm^{-1}, we have

at 444°K $\sigma(2) = 6.76 \times 10^{-6}$ ohm^{-1} cm^{-1}

at 285°K $\sigma(2) = 5.18 \times 10^{-8}$ ohm^{-1} cm^{-1}

at 170°K $\sigma(2) = 5.39 \times 10^{-12}$ ohm^{-1} cm^{-1}

The measured value of conductivity at the corresponding temperatures are

at 444°K $\sigma = 2.1 \times 10^{-3}$ ohm^{-1} cm^{-1}

at 285°K $\sigma = 5.89 \times 10^{-7}$ ohm^{-1} cm^{-1}

at 170°K $\sigma = 3.55 \times 10^{-13}$ ohm^{-1} cm^{-1}

By comparing these results, we can conclude that the in-band conduction is the dominated conduction mechanism at high temperature (444°K to about 300°K), the contribution of the near band edge hopping process became important at about 300°K; and at 170°K, the conductivity may well be contributed by both transport mechanisms. Since the evaluations based on the assumed values of ΔW_1, ΔW_2, σ_1, and σ_2, the values

calculated can only be used as a rough estimation of the contribution to the conduction from these transport mechanisms. The conclusion deduced from these evaluations is shown schematically in Fig. 4.6.

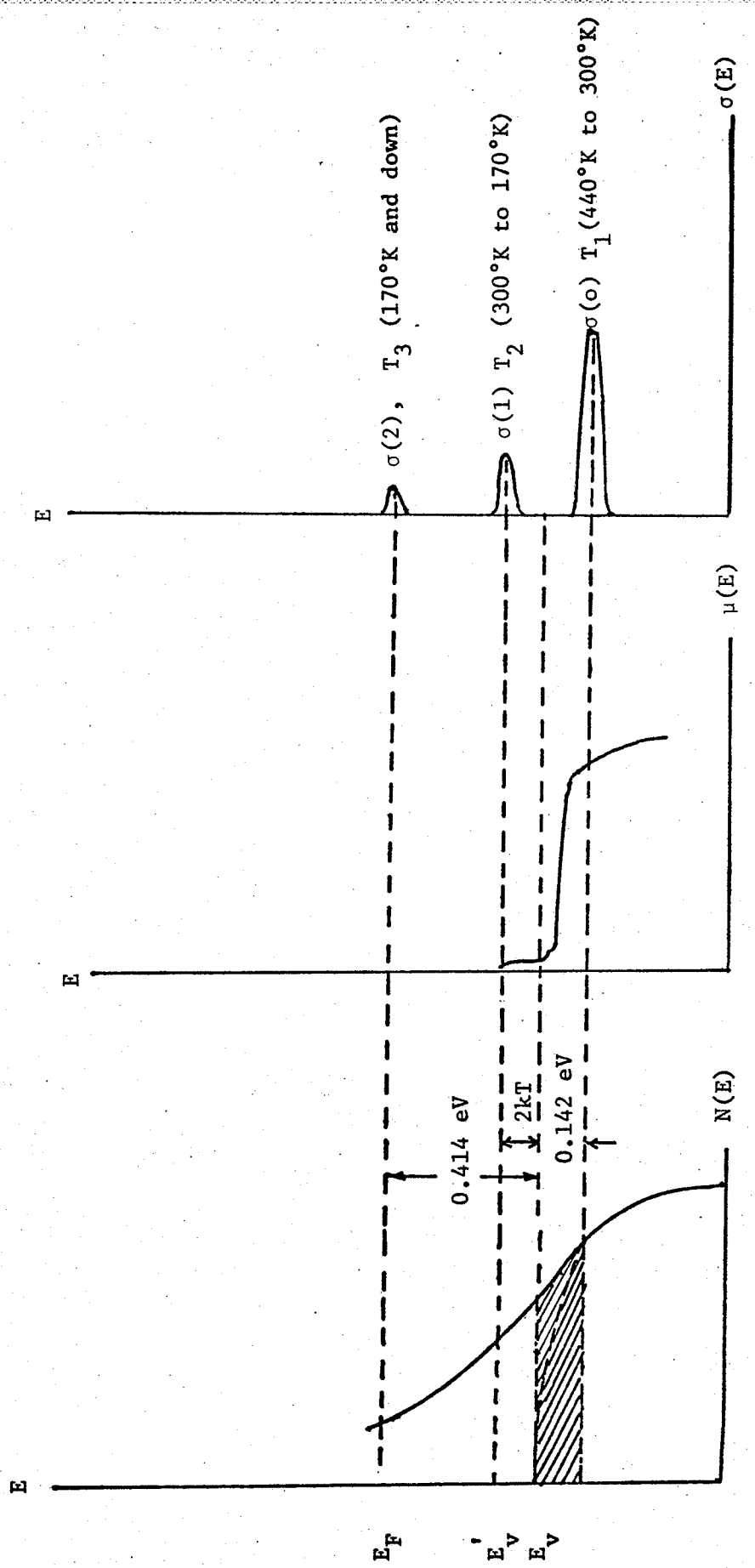

Fig. 4.6. The energy distribution of the density of states, the mobility, and the conductivity. $\sigma(o)$, $\sigma(1)$, $\sigma(2)$ correspond to the contribution of in-band conduction, the hopping near band edge and the hopping to the nearest neighbors near E_F.

CHAPTER 5

CONCLUSIONS

On the basis of the experimental results of dc conductivity and thermoelectric power (TEP), the following conclusions can be drawn:

1. The dc conductivity of Ge_{10} Si_{12} As_{30} Te_{48} increases experimentally with increasing temperature in the temperature region from 170°K to 444°K; the activation energy deduced from this temperature dependence ranging from 0.556 eV to 0.505 eV; and the associated pre-exponential factors from 4.25×10^3 ohm^{-1} cm^{-1} to 2.55×10^2 ohm^{-1} cm^{-1}, respectively.
2. The hole carriers are dominant in the conduction (exhibiting a p-type conduction).
3. The TEP decreases linearly with increasing temperature with an activation energy of about 0.414 eV.
4. The temperature factor of the activation energy is about the same order of k.
5. The hole mobility in the high temperature region (440°K to 286°K) increases exponentially with increasing temperature an activation energy deduced in this temperature region being about 0.142 eV.
6. The conduction mechanisms in the temperature range investigated is mainly due to in-band conduction but the contributions of hopping near the valence band edge is also significant at about room temperature. In the low temperature region (from 170°K to 210°K) both in-band conduction, hopping conduction near the band edge, and hopping conduction amongst localized states to the nearest neighbors play an important role in the conduction processes.

REFERENCES

Anderson, P.W., Phys. Rev. 111 (1958) 1029.

Baynton, P.L., Rawson, H. and Strauworth, J.E., J. Electrochem. Soc., 104 (1957) 231.

Bonch-Brukvich, V.L., J. Non-cryst. Solids, 4 (1970) 410.

Beyer, W. and Stuke, J., J. Non-cryst. Solids 8-10 (1972) 324.

Boer, K.W., Phys. Stat. Sol, 34 (1969) 721.

Boer, K.W., Phys. Stat. Sol., 34 (1969) 733.

Boer, K.W., J. Non-cryst. Solids, 2 (1970) 444.

Boer, K.W., J. Non-cryst. Solids, 4 (1970) 583.

Cohen, M.H., J. Non-cryst. Solids, 2 (1970) 432.

Cohen, M.H., J. Non-cryst. Solids 4 (1970) 391.

Cohen, M.H., Fritzsche, H., and Ovshinsky, S.R., Phys. Rev. Lett., 22, (1969) 1065.

Cutler, M. and Mott, N.F., Phys. Rev., 181, (1969) 1336.

Clark, A.H., Phys. Rev. 154 (1967) 750.

Clark, A.H., J. Non-cryst. Solids, 2 (1970) 52.

Chopra, K.L and Bahl, S.K., J. Appl. Phys., 40 (1969) 4171.

Davis, E.A., J. Non-cryst. Solids, 4 (1970) 107.

Davis, E.A. and Shaw, R.F., J. Non-cryst. Solids, 2 (1970) 406.

Edwards, S.F., J. Non-cryst. Solids, 4 (1970) 417.

Fagen, E.A., and Fritzsche, H., J. Non-cryst. Solids, 2 (1970) 170.

Fritzsche, H., J. Non-cryst. Solids, 6 (1971) 49.

Grigorovici, R., Croitbu, N. and Devenyi, A., Phys. Stat. Sol., 16 (1966) K143.

Grigorovici, R., J. Non-cryst. Solids, 1 (1969) 303.

Hindley, N.K., J. Non-cryst. Solids, 5 (1970) 17.

Hindley, N.K., J. Non-cryst. Solids, 5 (1970) 31.

Hurst, C.H. and Davis, E.A., J. Non-cryst. Solids, 8 - 10 (1972) 316.

Hill, R.M., Phil. Mag., 4P2 (1971) 1307.

Hill, R.M., Phil. Mag., 23 (1971) 59.

Ioffe, A.F. and Regel, A.R., Prog. Simicond. 4 (1960) 237.

Kolomiets, B.T., Phys. Stat. Sol., 7 (1964) 713.

Kolomiets, B.T. and E.M. Raspopova, Soviet Phys. - Semicond. 5, No. 8 (1972) 1346.

Lifshitz, I.M., Adv. Phys., 13 (164) 483.

Mott, N.F. and Davis, E.A., Electronic Processes in Non-crystalline Materials, Clarendon Press, Oxford (1971).

Mott, N.F., Adv. Phys., 16 (1967) 49.

Mott, N.F., J. Non-cryst. Solids, 1 (1968) 1.

Mott, N.F., Phil. Mag., 20 (1969) 1

Mott, N.F., Phil. Mag., Paper VI, 24 (1971) 1.

Male, J.C., Electronics Lett., 6 (1970) 91.

Marshall, J.M. and Miller, G.R., Phil. Mag., 27 (1973) 1151.

Mette, H. and Loscoe, C., Rev. Scientific Instru., 37 No. 11 (1966) 1957.

Miller, A. and Abrahams, E., Phys. Rev., 120 (1960) 745.

Nguyen Van Dong, J. Non-cryst. Solids, 12 (1973) 161.

Nagels, P., Callaerts, R., Denayer, M. and De Coninck, J. Non-cryst. Solids 4 (1970) 295.

Ninomiya, Y., Nakamua, Y. and Shunoji, J. Non-cryst. Solids, 17 (1975) 231.

Osmun, J.W., Bull. Am. Phys. Soc., 14 (1969) 311.

Ormondroyd, R.F., Allison, J. and Thompson, M.J., J. Non-cryst. Solids, 15 (1974) 310.

Putley, E.H., The Hall effect and Related Phenomena, (1960) Butterworth, London.

Pathria, R.K., Statistical Mechanics, Pergamn Press (1973).

Pearson, A.D., Modern Aspects of the Vitreous State, Vol. 3, (1964) Butterworth, Washington.

Pearson, A.D., J. Non-cryst. Solids, 2 (1970) 1.

Roilos, M., J. Non-cryst. Solids, 6 (1971) 5.

Rockstad, H.K., J. Non-cryst. Solids, 2 (1970) 192.

Rockstad, H.K., Flasck, R. and Iwasa, S., J. Non-cryst. Solids, 8 - 10 (1972) 326.

Roosbrueck, W.V. and Casey, Jr., H.C., Phys. Rev. B5 (1972) 2154.

Strunk, R., J. Non-cryst. Solids, 12 (1973) 168.

Spear, W.E., J. Non-cryst. Solids, 1 (1969) 197.

Tauc, J. and Menth, A., J. Non-cryst. Solids 8 - 10 (1972) 569.

Uphoff, H.L. and Healy, J.H., J. Appl. Phys., 32 (1961) 950.

Walley, P.A. and Jonscher, A.K., Thin Solid Films, 1 (1968) 367.

Walley, P.A., Thin Solid Films, 2 (1968) 327.